iScience

CellPress

Article

Clam Genome Sequence Clarifies the Molecular Basis of Its Benthic Adaptation and Extraordinary Shell Color Diversity

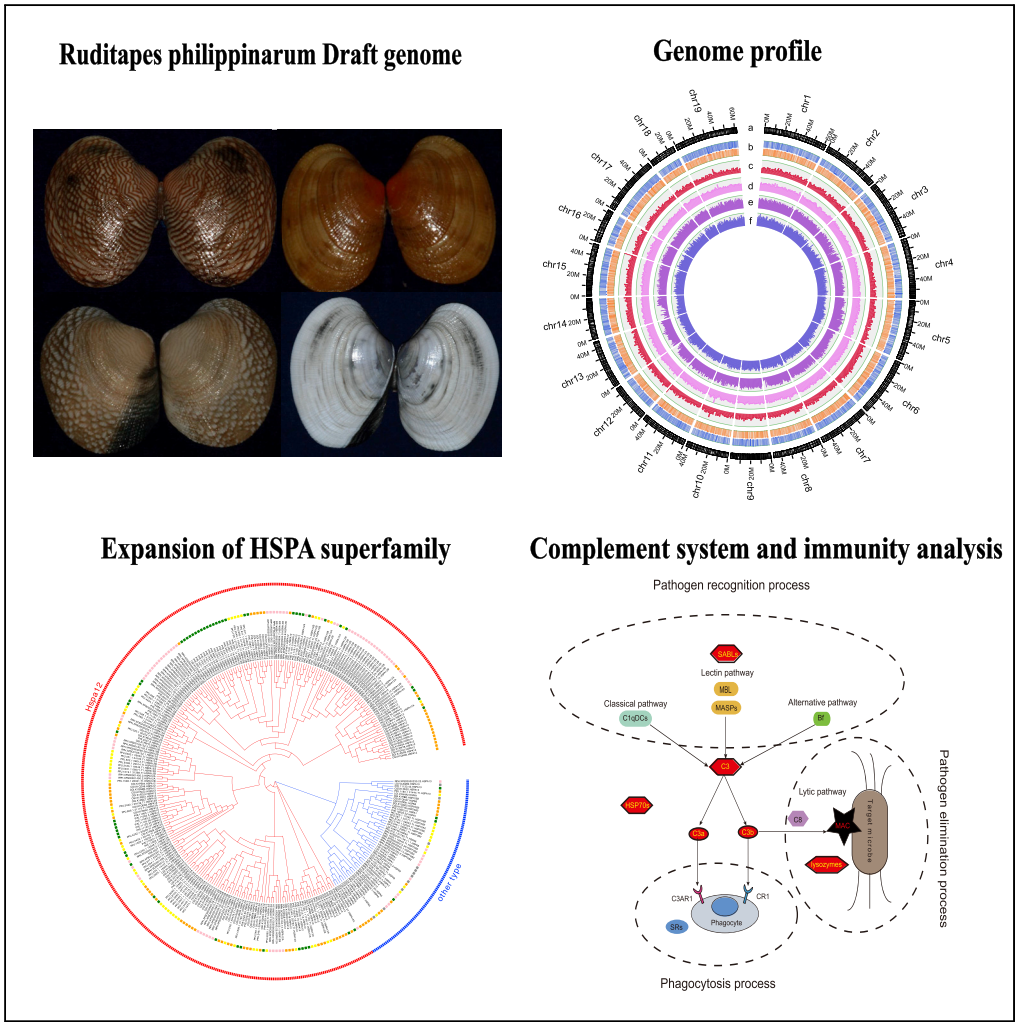

Xiwu Yan, Hongtao Nie, Zhongming Huo, ..., Md. Golam Rbbani, Guangjian Liu, Dongdong Li

yanxiwu@dlou.edu.cn (X.Y.)
htnie@dlou.edu.cn (H.N.)
liuguangjian@novogene.com (G.L.)

HIGHLIGHTS

We present a new genome assembly of the Manila clam *Ruditapes philippinarum*

Analysis of gene family expansions and transcriptome characterization were conducted

Tyr and mitf genes were potentially involved in shell color patterns of Manila clam

Expansion of GPCRs and immune-related genes were found in *R. philippinarum*

Yan et al., iScience 19, 1225–1237
September 27, 2019
https://doi.org/10.1016/j.isci.2019.08.049

iScience

CellPress

Article

Clam Genome Sequence Clarifies the Molecular Basis of Its Benthic Adaptation and Extraordinary Shell Color Diversity

Xiwu Yan,[1,3,4,*] Hongtao Nie,[1,3,*] Zhongming Huo,[1,3] Jianfeng Ding,[1,3] Zhenzhen Li,[2,3] Lulu Yan,[1] Liwen Jiang,[1] Zhengqiang Mu,[1] Huamin Wang,[1] Xiangyu Meng,[1] Peng Chen,[1] Mengyan Zhou,[2] Md. Golam Rbbani,[1] Guangjian Liu,[2,*] and Dongdong Li[1]

SUMMARY

***Ruditapes philippinarum* is an economically important bivalve with remarkable diversity in its shell coloration patterns. In this study, we sequenced the whole genome of the Manila clam and investigated the molecular basis of its adaptation to hypoxia, acidification, and parasite stress with transcriptome sequencing and an RNA sequence analysis of different tissues and developmental stages to clarify these major issues. A number of immune-related gene families are expanded in the *R. philippinarum* genome, such as *TEP*, *C3*, *C1qDC*, *Hsp70*, *SABL*, and *lysozyme*, which are potentially important for its stress resistance and adaptation to a coastal benthic life. The transcriptome analyses demonstrated the dynamic and orchestrated specific expression of numerous innate immune-related genes in response to experimental challenge with pathogens. These findings suggest that the expansion of immune- and stress-related genes may play vital roles in resistance to adverse environments and has a profound effect on the clam's adaptation to benthic life.**

INTRODUCTION

Bivalves are represented by approximately 20,000 species, distributed throughout aquatic habitats (Daniel, 2013). The Manila clam, *Ruditapes philippinarum*, is a bivalve mollusk with a worldwide distribution and important commercial, culinary, and ecological value. The production of *R. philippinarum* reached over 4.0 million tons, equivalent to 3.7 million USD, in 2015 (FAO, 2017). As a filter-feeding animal living buried in sediment, *R. philippinarum* is an important "sentinel" species used to assess the quality of the marine environment (Milan et al., 2011). Benthic bivalves play important roles in food chains, including as food for humans, and most benthic bivalves are critical in bioturbation, bioirrigation, and the breakdown of organic matter (Norkko and Shumway, 2011). However, massive mortality in the Manila clam has been reported arising from parasitic infections, which has severely affected the Manila clam industry (Choi et al., 2002; Pretto et al., 2014). Moreover, ocean acidification, increased water temperatures, and hypoxic events are increasing worldwide problems (Steckbauer et al., 2015). The molecular mechanisms underlying the tolerance of benthic organisms for diverse biotic and abiotic factors, such as parasites, ocean acidification, and hypoxia, have received much attention in recent years (Lim et al., 2006; Shimokawa et al., 2010; Zhao et al., 2018; Kodama et al., 2018).

Bivalve mollusks have a biphasic life cycle, in which planktonic larvae (trochophores and veligers) settle (as pediveliger larvae) and undergo metamorphosis (to the juvenile stage). The transition of benthic bivalves from a pelagic to a benthic lifestyle during their early development, their burrowing to avoid predation, and their tolerance of hypoxic environments have been attractive characteristics for research (Tamai, 1993; Kodama et al., 2018). However, knowledge of the underlying molecular mechanisms that regulate these processes is still very limited (Findlay and Battin, 2016). The Manila clam is an excellent marine model system, with a robust and multifaceted immune system (Dyachuk, 2016). The immune system of bivalves relies on the recognition of conserved pathogen-associated molecular patterns shared by broad classes of microorganisms, which allows the bivalves to successfully defend themselves against infection (Gestal et al., 2008; Ki et al., 2006; Song et al., 2010). Sediment is a specific habitat of bivalves, with characteristic microbial diversity, low input of sunlight, and a low concentration of oxygen (Wang et al., 2012). Benthic bivalves live in sediment and play important roles in natural biochemical cycles and in the material exchanges between water bodies and sediments (Vaughn and Hakenkamp, 2001). How benthic bivalves adapt to and survive in such hypoxic and pathogen-rich environments is of fundamental interest.

[1]Engineering and Technology Research Center of Shellfish Breeding in Liaoning Province, College of Fisheries and Life Science, Dalian Ocean University, Dalian 116023, China

[2]Novogene Bioinformatics Institute, Beijing 100083, China

[3]These authors contributed equally

[4]Lead Contact

*Correspondence: yanxiwu@dlou.edu.cn (X.Y.), htnie@dlou.edu.cn (H.N.), liuguangjian@novogene.com (G.L.)

https://doi.org/10.1016/j.isci.2019.08.049

Despite its burrowing lifestyle, *R. philippinarum* displays a large range of shell colors and patterns (Protas and Patel, 2008; Zhang and Yan, 2010). The Manila clam has several different shell colors, including white, zebra, and orange in its natural habitat (Figure S1), and it has been selected over several generations for high stress resistance and distinctive shell color with selective breeding programs (Zhang and Yan, 2010). Previous experimental crosses have shown that shell color has a genetic basis in the Manila clam (Peignon et al., 1995). Color is one of the most conspicuous phenotypic traits in *R. philippinarum*, and the diverse colors of molluscan shells are generally believed to be determined by the presence of biological pigments (Mann and Jackson, 2014; Lemer et al., 2015; Feng et al., 2018). Several studies have been conducted of the physiological, biochemical, and molecular responses to different types of biotic and abiotic stress in different shell color strains of the Manila clam (Zhang and Yan, 2010; Nie et al., 2017a, 2017b). In recent years, RNA sequencing (RNA-seq) has been used to identify the genes differentially expressed in the differently colored shells of several bivalves (Sun et al., 2015; Feng et al., 2015; Yue et al., 2015). However, the genes potentially responsible for shell color formation and variation in strains of *R. philippinarum* are still largely unknown. The expression of genes for tyrosinase (*Tyr*) and melanogenesis-associated transcription factor (*Mitf*) is responsible for the production of melanin from tyrosine, promoting melanin production and stimulating pigmentation (Krumholz et al., 2011). In mollusks, tyrosinase is secreted and appears to contribute to shell pigmentation and melanin synthesis, which can also physically encapsulate pathogens, and is therefore, an important component of the immune system (Cerenius et al., 2008).

The main goals of this study were to provide a robust reference genome for the Manila clam and to analyze its transcriptomic responses to various stimuli and different ontogenetic stages. Here, we report the whole genome sequence of the Manila clam and its *de novo* assembly and a comparative analysis with a Korean strain of the Manila clam (Mun et al., 2017). We also examined the expression of pigmentation-related genes (*Tyr* and *Mitf*), immune pathways, and defense mechanisms in the Manila clam. To better understand these biological issues, RNA-seq analyses of hypoxia-challenged, acidification-exposed, and parasite-infected clams were performed, as were RNA-seq analyses of different shell color strains and developmental stages of the Manila clam. This study provides clues to the molecular mechanisms underlying the shell pigmentation, immune defenses, and resistance to different stresses in this clam. Comparative genomic analyses of gene expansion, contraction, and positive selection in *R. philippinarum* and *Lottia gigantea* (Simakov et al., 2013), *Crassostrea gigas* (Zhang et al., 2012), *Pinctada fucata* (Takeuchi et al., 2012), and *Patinopecten yessoensis* (Wang et al., 2017) also identify important genetic differences among these species and provide insights into the molecular basis of adaptation to a benthic lifestyle in clams.

RESULTS

Genome Characterization

The genome of *R. philippinarum* is shown in Figure 1A. The Manila clam genome has a high level of heterozygosity and an estimated size of 1.32 Gb (Table S1 and Figure S2). To reduce the heterozygosity, genomic DNA isolated from an inbred individual (six generations, 2.0% estimated heterozygosity) (Figure S1D) was used for whole-genome shotgun sequencing (286.1 Gb of high-quality paired-end data and 135.1 Gb of mate-pair data; Table S2 and Figure S3). The *R. philippinarum* assembly comprised 30,811 scaffolds with an N50 length of 345 kb and a total length of 1.12 Gb (Table S3). The heterozygosity of the assembly was reduced to 1.038%, compared with that of a wild-type individual (1.69%) (Table S4). Evaluation of the genome showed the completeness of the assembly (Tables S5–S7). A total of 233 CEGMA (Core Eukaryotic Genes Mapping Approach) core genes with a ratio of completeness of 93.95% (Table S8), together with 91.0% complete and 3.9% fragmented Metazoa BUSCO (Benchmarking Universal Single-Copy Orthologs) orthologs (Table S9), were identified in the assembled genome, indicating the high degree of completeness of the gene regions. Repetitive regions comprised ~38.30% of the *R. philippinarum* assembly (Table S10, and Figure S4), and combined transposable elements were predicted to constitute 35.8% of the *R. philippinarum* genome (Table S11). Transcriptome-based, *ab initio*, and homology-based predictions identified 27,652 protein-coding genes (Table S12), a similar number to other Lophotrochozoa genomes (Table S13 and Figure S5). Of these, 24,570 (88.85%) were annotated based on various public databases (Table S14), with the best BLASTp hits in the SwissProt, TrEMBL, and NCBI nonredundant (NR) protein databases. Gene domain annotations were made by searching the InterPro database. All genes were functionally annotated by their alignment against Kyoto Encyclopedia of Genes and Genomes (KEGG) and Gene Ontology (GO) terms. Noncoding RNA was also annotated (Table S15).

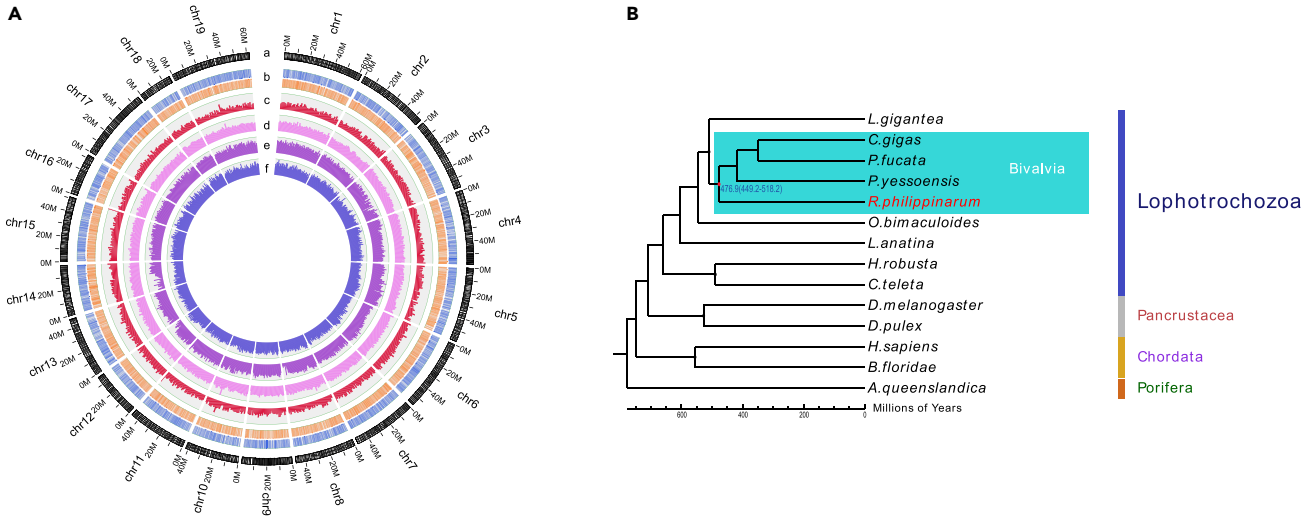

Figure 1. Genome Landscape and Phylogenetic Analysis of *R. philippinarum*

(A) From outer to inner circles: a marker distribution on 19 chromosomes at the Mb scale; b gene distribution on each chromosome; blue lines indicate genes on the forward direction strand, and yellow lines indicate genes on the reverse direction strand; c GC content within a 1-Mb sliding window; d repeat content within a 1-Mb sliding window; e SNP density of the inbreed offspring; f SNP density of the wild sample.

(B) Phylogenetic tree among 14 species. The split of *R. philippinarum* was estimated at 476.9 million years ago.

Comparative Analysis of *R. philippinarum* (Rph) and Korean Clam (Hrph) Genomes

We compared the genomic statistics for Rph and Hrph (Table 1). The contig N50 for Rph was 28,111 bp, whereas that for Hrph was 6,520 bp. The complete BUSCO (C) ratio of the Rph genome was 92.2%, which was much higher than that of the Hrph genome (69.5%). The number of protein-coding genes in Rph was 27,652, whereas that in Hrph was 108,034, and the complete BUSCO (C) ratios of the genes were 91.0% and 81.5%, respectively (Table 1). There was about 67% collinearity between the Rph and Hrph genomes. To analyze the gene families, the genes of Hrph were filtered from 108,034 to 19,776. A gene family cluster analysis was performed between Rph, Hrph, and six other species, including *C. gigas*, *L. gigantea*, *P. fucata*, *Patinopecten yessoensis*, *Octopus bimaculoides*, and *Lingula anatina*, and 436 orthologous gene families were shared among these species. Rph shared 1,266 orthologous gene families with the other species, excluding Hrph. Of these 1,266 genes, 1,240 were not annotated and 26 genes were annotated in more than one copy in the Hrph genome, and 1,246 were annotated in the collinear regions of the Rph and Hrph genomes. Hrph shared 56 orthologous gene families with other species, excluding Rph. Of the 56 genes, 16 genes were not annotated and 40 genes were annotated in more than one copy in the Rph genome, and 48 genes were annotated in the collinear regions of the Rph and Hrph genomes. Compared with Hrph, 7 expanded and 78 contracted gene families were detected in Rph with Fisher's exact test (Table S16). A GO enrichment analysis of the expanded gene families in Rph, relative to Hrph, revealed that active transmembrane transporter activity, neurotransmitter transport, hydrolase activity, and scavenger receptor activity are involved in their immune functions and ecological adaptation (Table S16).

Comparative Genome Analysis of the Gene Families

The results of a gene family cluster analysis of *R. philippinarum* and other 13 species are shown in Figure S6. Compared with four other Mollusca species (*C. gigas*, *L. gigantea*, *P. fucata*, and *Patinopecten yessoensis*), *R. philippinarum* has 1,582 unique gene families and shares 6,975 gene families with other species (Figure S7, Tables S17 and S18). A phylogenetic tree was constructed using 288 shared single-copy orthologues of 14 species (Figure 1B). As the closest bivalve clade to the class Gastropoda (*L. gigantean*), *R. philippinarum* was estimated to have split from it about 476.9 million years ago (Figure 1B). Compared with the four other Mollusca species, 2,197 expanded and 3,943 contracted gene families were identified in *R. philippinarum* with Fisher's exact test (Tables S19 and S20–S22), and 29 positively selected genes were detected in the *R. philippinarum* genome as the foreground branches and genes of four other Mollusca species as background branches (Tables S23 and S24). GO and KEGG enrichment analyses of the expanded genes revealed that they are involved a number of immune-related pathways in

Type	Rph	Hrph
Estimated genome size (Gb)	1.32	1.37
Assembly total length (bp)	1,122,973,377	1,078,771,101
Sequencing depth	320.63	74.2
Contig N50 (bp)	28,111	6,520
Scaffold N50 (bp)	56,467,786	119,518
Average contig length (bp)	12,041	3,186
Max contig length (bp)	249,659	80,451
Average scaffold length (bp)	56,456,578	80,439
Max scaffold length (bp)	204,629,219	1,050,406
Number of contig > 2 Kb	61,395	121,896
Number of scaffolds > 2 Kb	19	13,318
Genome BUSCO assessment	C:92.2%[S:90.3%,D:1.9%],F:1.6%,M:6.2%,n:978	C:69.5%[S:66.6%,D:2.9%],F:11.2%,M:19.3%,n:978
Repeat percentage	38.29	26.38
Gene models number	27,652	108,034
Average gene length (bp)	12,875	5,117
Average number of exons per gene	7.30	4.17
Average exon length (bp)	200.30	232
Average number of introns per gene	6.29	3.17
Average intron length (bp)	1,697.30	1,230
Gene BUSCO assessment	C:91.0%[S:89.3%,D:1.7%],F:3.9%,M:5.1%,n:978	C:81.5%[S:58.9%,D:22.6%],F:13.2%,M:5.3%,n:978

Table 1. Comparative Analysis between the Current Genome of Manila Clam and the Genome of Korean Manila Clam
Rph, the current genome of Manila clam; Hrph, the genome of Korean Manila clam.

R. philippinarum, including in the defense response to scavenger receptor activity, cytokine activity, apoptotic process, G-protein-coupled receptor activity, sulfotransferase activity, tumor necrosis factor (TNF) receptor binding, neuropeptide signaling pathway (Table S25), complement and coagulation cascades, phagosome, Toll-like receptor signaling pathway, NF-κB signaling pathway, TNF signaling pathway, and PI3K–AKT signaling pathway (Table S26).

Differential Expression of *Tyr* and *Mitf* Genes in Manila Clam

Manila clams are capable of producing an extraordinary diversity of shell color patterns. We examined the molecular processes of the melanogenesis and tyrosine metabolism pathways, which are involved in pigment synthesis. Tyrosinase (encoded by *Tyr*) is a crucial enzyme in the process of melanin synthesis, and the *Tyr* genes are regulated by a melanogenesis-associated transcription factor (encoded by *Mitf*). In this study, transcriptomic and gene expression analyses of the *Tyr* and *Mitf* genes in four shell color strains of *R. philippinarum* were conducted with RNA-seq and quantitative PCR (qPCR) (Figure 2). In total, 21 *Tyr* genes and 12 homologues of the *Mitf* gene were identified in the *R. philippinarum* genome. Most of the *Mitf* mRNAs were upregulated in the orange strain (O), and three of them were uniquely and strongly expressed in O compared with the other three color strains (Figure 2A). To confirm the differential expression of *Tyr* and *Mitf* in the different shell color strains, six *Tyr* and seven *Mitf* genes were further evaluated with RT-qPCR in four different shell color strains of *R. philippinarum*, and all of them were differentially expressed in the four shell color strains (Figure 2). All seven *Mitf* genes were upregulated in the mantle of the O strain, compared with the zebra strain, and three *Mitf* genes (*Mitf1*, *Mitf2*, and *Mitf5*) were upregulated in the mantle of the white zebra (WZ) strain (Figure 2A). An RNA-seq analysis was conducted in the different developmental stages of *R. philippinarum*, including the trochophore, D-shaped larval, umbo-veliger larval, spat, early juvenile before shell pigmentation, and late juvenile after shell

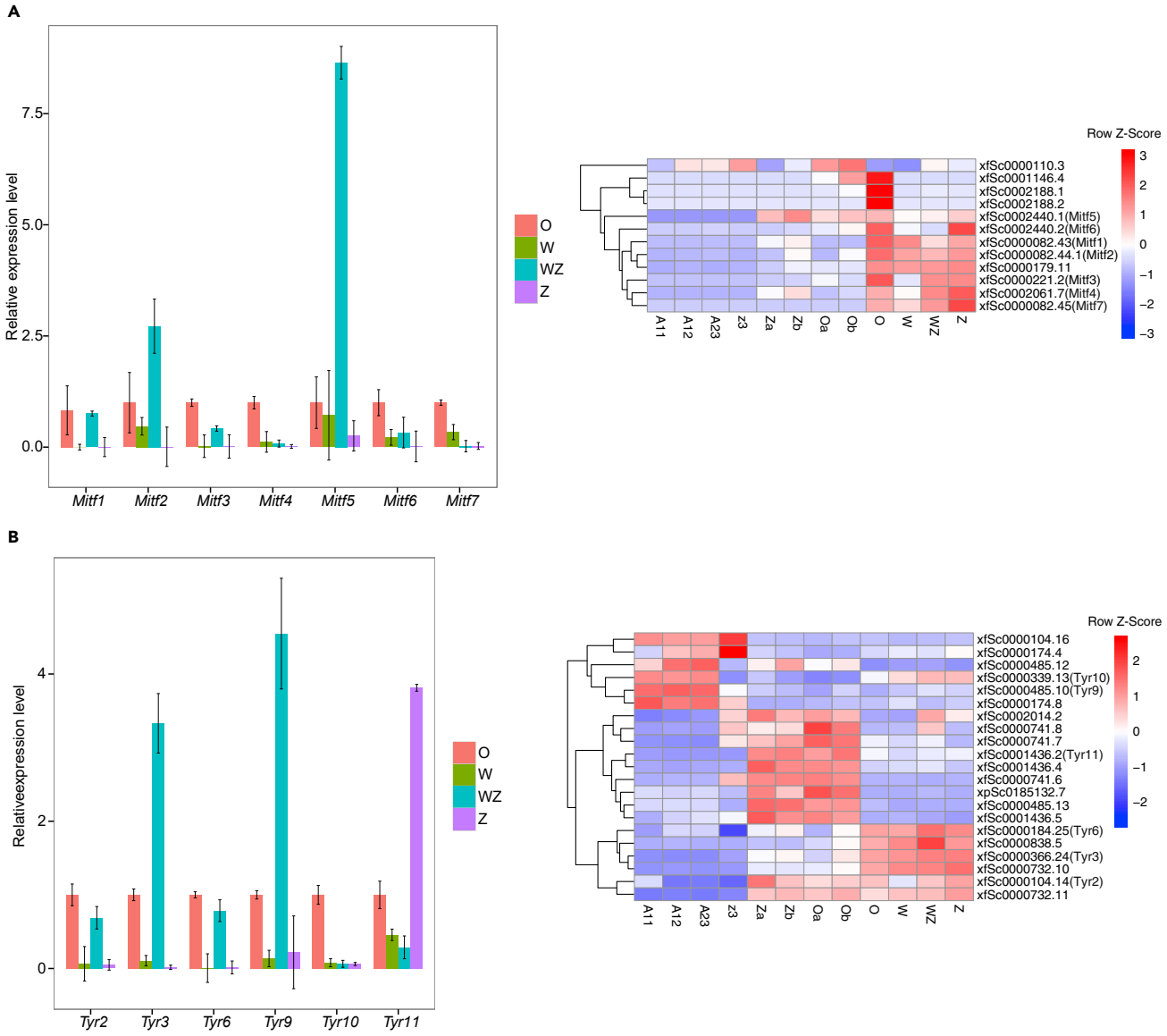

Figure 2. The Expression of Key Genes Impacting Shell Color Patterns in *R. philippinarum* and Evolutionary Analysis of Tyr Genes

(A) RNA-seq hierarchical clustering of Mitf genes at four different developmental stages, at noncolored and colored developmental stages in two different shell color strains, and in four different shell color strains, as well as RT-qPCR expression of seven Mitf genes in four different shell color strains.

(B) RNA-seq hierarchical clustering of Tyr genes at four different developmental stages, at noncolored and colored developmental stages in two different shell color strains, and in four different shell color strains, as well as RT-qPCR expression of six Tyr genes in four different shell color strains. The abbreviations include trochophora (A11), D-shaped larvae (A12), umbo larvae (A23), pediveliger larvae (z3), uncolored zebra clam (Za), colored zebra clam (Zb), uncolored orange clam (Oa), colored orange clam (Ob), Orange strain (O),White strain (W), White Zebra strain (WZ), and Zebra strain (Z).

pigmentation stages. The expression of four *Mitf* genes was upregulated between the early juvenile stage before shell pigmentation and the juvenile stage after shell pigmentation (Figure 2A). Interestingly, the *Tyr* gene family showed a distinctive expression pattern and stage-specific expression in pelagic larvae (trochophore, D-shaped larva, and umbo-veliger larva), benthic juveniles (early juvenile and late juvenile), and adult clams (Figure 2B).

Expansion of Immune-Related Genes in *R. philippinarum*

Compared with four other Mollusca species (*C. gigas*, *P. fucata*, *L. gigantea*, and *Patinopecten yessoensis*), a number of immune-related genes are expanded in *R. philippinarum*, including the thioester-containing

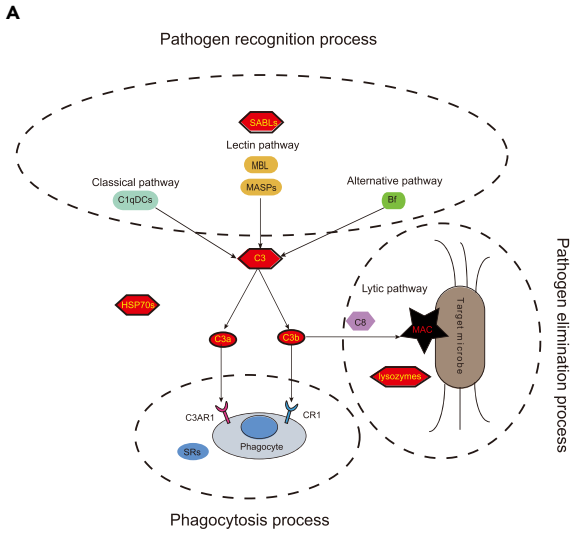
A
Pathogen recognition process
SABL
Lectin pathway
MBL
MASPs
Classical pathway
C1qDCs
Alternative pathway
Bf
C3
HSP70
Lytic pathway
C8
MAC
Target microbe
C3a
C3b
lysozymes
C3AR1
CR1
SRs
Phagocyte
Pathogen elimination process
Phagocytosis process

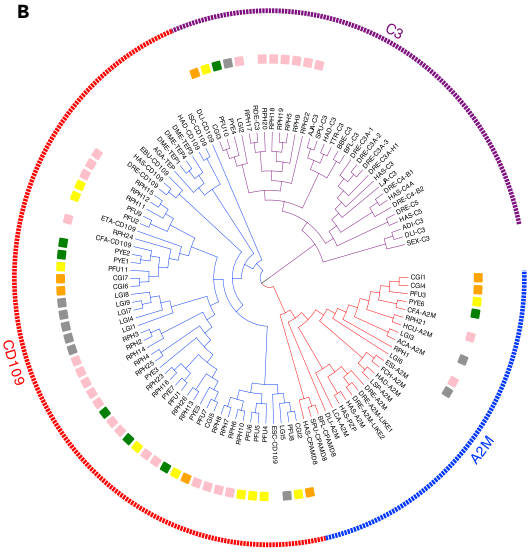
B
C3
CD109
A2M

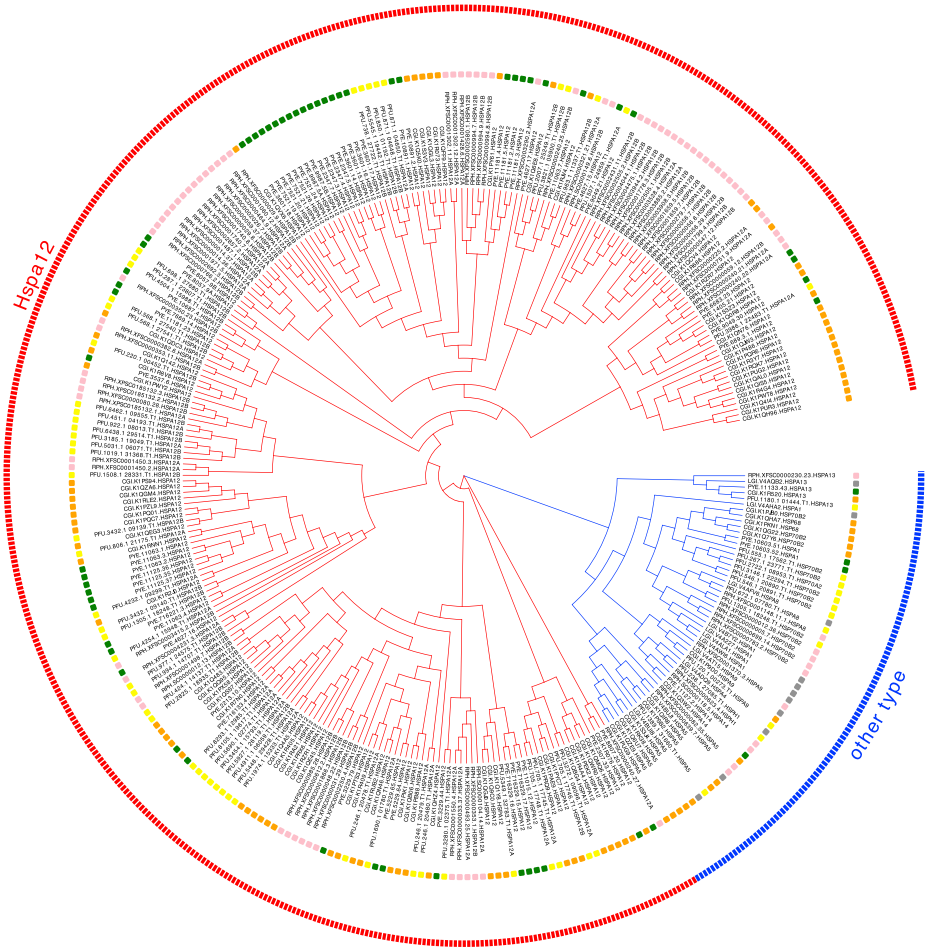
C
Hspa12
other type

Figure 3. Analysis of Immunity in *R. philippinarum*

(A) A schematic diagram depicting the complement system in *R. philippinarum*. Hexagons with bold black borders indicate gene families (*HSP70s, C3, SABLs,* and *lysozymes*) expanded in *R. philippinarum*. The pathogen recognition in *R. philippinarum* can be equipped with pathogen recognition receptors C1qDCs, Bf, and carbohydrate-binding lectins such as SABLs and MBL through three well-defined activation pathways—the classical, alternative, and lectin pathways. Then, the central complement component C3 was proteolytically activated by converting into fragments C3a and C3b. Upon proteolytic activation, C3b bonds covalently to the surface molecules of microbes using its intrachain thioester bond and initiates the formation of the membrane-attack complex (MAC), which can eliminate the invading pathogens by the lytic pathway. On the other hand, C3a and degraded C3b can be recognized by complement C3a receptor 1 (C3AR1) and complement component (3b/4b) receptor 1 (CR1) on phagocytes, respectively, which may induce the chemotaxis and opsonization of target cells. C1qDCs, C1q domain-containing proteins; SABLs, sialic acid-binding lectins; MBL, mannose-binding lectin; MASPs, Mannan-binding protein associated serine proteases; Bf, Factor B; C3, complement component 3; HSP70s, heat shock 70 kDa proteins; C8, complement component 8; SRs, scavenger receptor.

(B) Phylogenetic tree of TEP superfamily from selected organisms. The tree shows the three classic subgroups of the TEP superfamily, the C3 subgroup in purple, the alpha 2-macroglobulin protease inhibitors (A2M) in red, and the CD109/iTEPs subgroup in blue. The pink blocks, green blocks, yellow blocks, orange blocks and gray blocks indicate the genes of *R. philippinarum*, *P. yessoensis*, *P. fucata*, *C. gigas,* and *L. gigantea*. *R. philippinarum* has more genes of C3 and CD109/iTEPs subgroups (seven and seventeen, respectively) in comparison with *C. gigas*, *L. gigantea, P. fucata,* and *P. yessoensis*, which suggested a species-specific gene expansion in *R. philippinarum*. The abbreviations of species are: ACA, *Aplysia californica*; ADI, *Acropora digitifera*; AGA, *Anopheles gambiae*; AJA, *Apostichopus japonicas*; BBE, *Branchiostoma belcheri*; BFL, *Branchiostoma floridae*; CFA, *Chlamys farreri*; CGI, *Crassostrea gigas*; DLI, *Diadumene lineata*; DME, *Drosophila melanogaster*; DRE, *Danio rerio*; EBU, *Eptatretus burger*; ESC, *Euprymna scolopes*; ESI, *Eriocheir sinensis*; ETA, *Euphaedusa tau*; FCH, *Fenneropenaeus chinensis*; HAD, *Hasarius adansoni*; HAS, *Homo sapiens*; HCU, *Hyriopsis cumingii*; ISC, *Ixodes scapularis*; ICA, *Lethenteron camtschaticum*; LGI, *Lottia gigantea*; LJA, *Lethenteron japonicum*; LSP, *Limulus sp.*; PFU, *Pinctada fucata*; rde, *Ruditapes decussatus*; RPH, *Ruditapes philippinarum*; SEX, *Swiftia exserta*; SPU, *Strongylocentrotus purpuratus*; TTR, *Tachypleus tridentatus*.

(C) Phylogenetic tree of HSP70 family genes in *R. philippinarum*, *C. gigas*, *L. gigantea*, *P. fucata,* and *P. yessoensis*. The pink blocks, green blocks, yellow blocks, orange blocks, and gray blocks indicate the genes of *R. philippinarum*, *P. yessoensis*, *P. fucata*, *C. gigas*, and *L. gigantea*. All bivalve HSPA12 genes from *R. philippinarum*, *C. gigas*, *P. fucata*, and *P. yessoensis* are clustered with red blocks. Gene names in purple belong to *R. philippinarum*. The other clusters consisting of HSPA1, HSPA4, HSPA5, HSPA8, HSPA9, HSPA13, HSPA14, HSPH1, HSP70B2, and HSP68 are clustered with blue blocks.

proteins (*TEP*), complement component C3 (*C3*), C1q domain-containing proteins (*C1qDC*), lysozymes, sialic acid-binding lectin (*SABL*), and heat shock protein 70 (*Hsp70*) (Figure 3). These gene families expanded in *R. philippinarum* are enriched in complement and coagulation cascades, phagosome, and lytic pathways (Figure 3). Pathogen recognition in *R. philippinarum* can be attributed to pathogen recognition receptors C1qDCs, Bf, and carbohydrate-binding lectins, such as SABLs and mannan-binding lectin, through the complement pathways (Figure 3A).

Ruditapes philippinarum has the largest number of genes in the C3 and CD109/iTEP subgroups (7 and 17 members, respectively), compared with *C. gigas*, *L. gigantea*, *P. fucata*, and *Patinopecten yessoensis* (Table S27), suggesting species-specific gene family expansion in *R. philippinarum*. Phylogenetic analyses also indicated extensive expansion of the *Hsp70* genes from the *Hspa12* subfamily in *R. philippinarum* and also in the bivalve lineages (Figure 3C). The expansion of immune-related genes (*SABL*, *C3*, *C1qDC*, *lysozyme,* and *Hsp70*) provides evidence of an association between gene duplication and the organism's adaptation to pathogen-rich environments (Figure 4). The characteristics and expression of five complement *C3* genes (xfsc0000076.27, xfsc0000154.2, xfsc0000773.3, xfsc0000773.2, and xfsc0001170.6) were investigated in the blood and digestive gland of *R. philippinarum* at 3, 6, 12, 24, 48, 72, and 96 h after treatment with lipopolysaccharide (LPS), peptidoglycan (PGN), or polyinosinic–polycytidylic acid (poly[I:C]). All these complement *C3* genes were significantly upregulated in the immune responses of *R. philippinarum* to different pathogenic stimuli (LPS, PGN, and poly[I:C]) (Figure S8), indicating that the complement *C3* genes play critical roles in the immunity of the Manila clam.

RNA-Seq Analyses at Different Ontogenic Stages

To identify the key genes involved in the development and metamorphosis processes, RNA-seq analyses were conducted in the different ontogenic stages of *R. philippinarum*. The *Hox* gene clusters and their expression at different ontogenic stages are shown in Figure 5. The expression of 11 *Hox* genes was detected in 17 different stages, and the *Post1* and *Lox5* genes were expressed in the gastrula stage (Figure 5B). Most *Hox* genes were strongly expressed in the early trochophore stage, when the larvae begin to secrete the shell to coat and protect the embryo. The *Hox1*, *Post2*, *Hox3*, and *Lox4* genes were mainly expressed in trochophore and veliger larvae (Figure S9). In contrast, the *Hox2* and *Hox4* genes were strongly expressed in the umbo larvae (Figure 5B). The *Post2 and Lox4* genes were strongly expressed in the trochophore, veliger, and umbo larvae. The *Antp* and *Lox2* genes were strongly expressed in the umbo larvae, spats, and juveniles, whereas *Lox5* was strongly expressed in the gastrula stage (Figure 5B). The expression of immune-related genes *TEP* and *C3* was negligible throughout the different planktonic

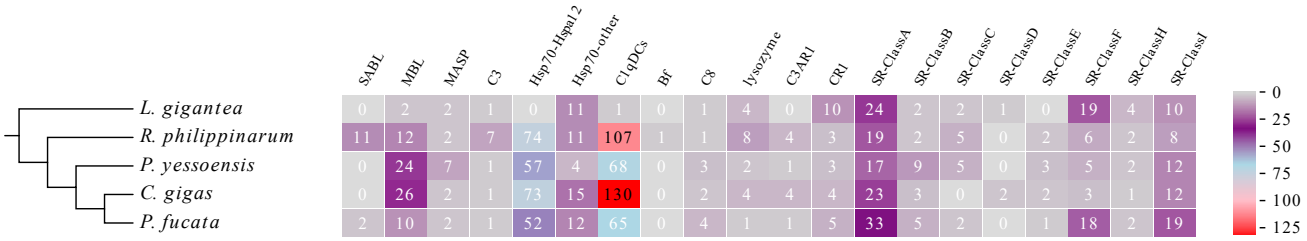

Figure 4. The Heatmap of the Immune-Related Genes Number in *L. gigantea*, *R. philippinarum*, *P. yessoensis*, *C. gigas*, and *P. fucata*

developmental stages (trochophore, D-shaped larva, and umbo-veliger larva) of *R. philippinarum*, but was induced during metamorphosis and increased significantly during the transition from the umbo-veliger larva to the spat stage (Figure S10). However, eight *Hsp70* genes were strongly expressed in the planktonic larval stages (trochophore, D-shaped larva, and umbo-veliger larva) compared with their expression in the benthic spat stage, whereas 40 *Hsp70* genes were strongly expressed in the spat stage during metamorphosis (Figure S11).

Transcriptomic Responses to Hypoxia, Acidification, and Parasites

We hypothesized that the expansion of the complement and immune-related genes plays a critical role in the resistance of the Manila clam to different stresses and in its benthic adaptation. The transcriptomic responses of the Manila clam to hypoxia, acidification, and parasites were analyzed to identify the complement- and immune-responsive genes. An RNA-seq analysis identified 102 differentially expressed genes (DEGs), including 75 upregulated genes and 27 downregulated genes, corresponding to 12 major physiological functions in the gills of *R. philippinarum* after exposure to hypoxia for 2 days (Table S28). The expression of hypoxia-responsive genes encoding Hsp70, C-type lectin, complement factor B-1 (*CFB*), Ikappa, melatonin receptor type 1A (*MRTA*), serine/threonine-protein phosphatase (*STP*), growth arrest, DNA damage-inducible protein (*GADD*), phosphoenolpyruvate carboxykinase (*PECKG*), and *Tyr* (xfSc0000104.14) was upregulated (Figure S12), whereas the expression of genes encoding TNF, NFX1, GTPase IMAP (*IMAP*), E3, and hemicentin was downregulated when analyzed with RT-qPCR after exposure to hypoxia for 0, 2, 5, or 8 days (Figure S12). These genes are implicated in different physiological pathways, including respiration and energy metabolism (carbonic anhydrase, *SLC2A1*) and antioxidant and immune defense (*CFB*, *C-type lectins*, *Hsp70*, *lysozyme*, *Tyr*, *TNF*, *ANKK1*, *IκB*, *GPx*).

To confirm the DEGs identified in clams under acidic conditions, 11 genes (six upregulated and five downregulated) were selected from the DEGs in several canonical pathways of interest and analyzed with RT-qPCR (Figure S13). A number of vital complement- and immune-responsive genes were significantly differentially expressed, including complement *C1q*, *SABL*, *C-type lectin*, *Hsp70*, and *CYP450*. An RNA-seq analysis of clams infected with digenetic trematodes identified 460 DEGs, including 416 upregulated and 44 downregulated genes (Table S29). Eleven candidate genes associated with immune, antioxidant, and molecular chaperone functions were chosen from the DEGs to confirm their expression levels with qPCR (Figure S14). In the infected clams, the expression of complement *C1q* and *C-type lectin* was significantly upregulated in the mantle and gonad. Expression of the *CYP450* gene was significantly downregulated in the gills but significantly upregulated in the mantle and gonad. The expression of inhibitor of apoptosis (*IAP*) and glutathione S-transferase (*GST*) was significantly elevated in the three tissues (Figure S14). The expression of *Hsp70* was significantly elevated in the gills of *R. philippinarum* after 2 and 5 days of hypoxia and after 12 h of acidification stress (both $p < 0.05$). A transcriptomic analysis of clams exposed to the parasite revealed that the expression of *Hsp70* was significantly increased ($p < 0.05$) in three tissues tested, including the gill, mantle, and gonad (Figure S14). Overall, the RNA-seq analysis revealed that the expanded *Hsp70* genes are involved in multistress resistance in *R. philippinarum*.

Expansion of the G-Protein-Coupled Receptor-Related Genes

G-protein-coupled receptors (GPCRs) were enriched in the unique and expanded genes of *R. philippinarum*. The numbers of genes containing the seven-transmembrane-associated domain in *R. philippinarum*, *Patinopecten yessoensis*, *P. fucata*, *C. gigas*, and *L. gigantea* were 858, 463, 533, 606, and 385, respectively (Table S30). Compared with the four other Mollusca species (*C. gigas*, *P. fucata*, *L. gigantea*, and *Patinopecten yessoensis*), the number of GPCR-related genes was expanded in

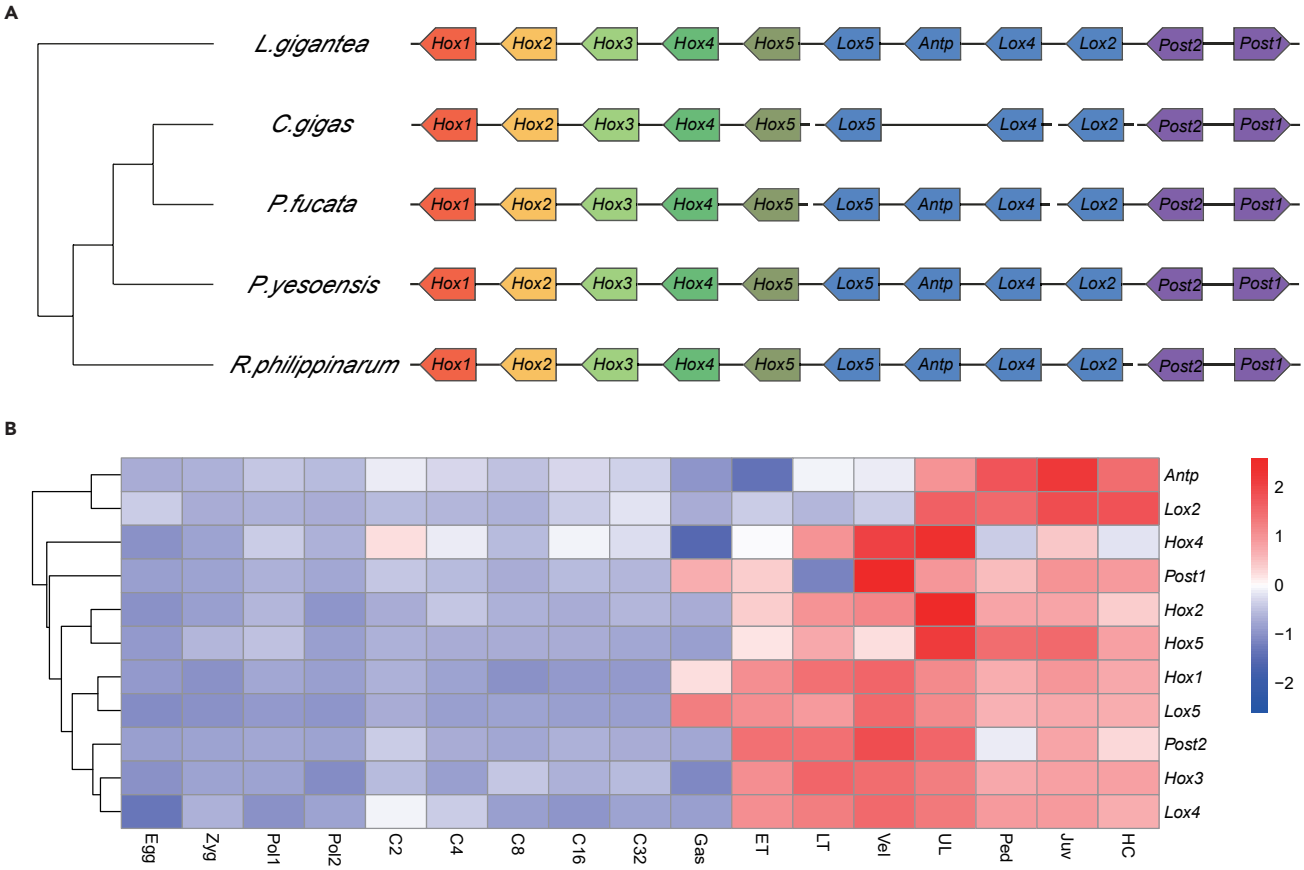

Figure 5. Hox Genes Clusters and the Expressions at Different Developmental Stages in *R. philippinarum*

(A) Clustering of Hox genes in *R. philippinarum* (Rph), *C. gigas* (Cgi), *L. gigantea* (Lgi), *P. fucata* (Pfu), and *P. yessoensis* (Pye) genomes. The relative position and orientation of the genes are indicated.

(B) RT-qPCR hierarchical clustering of Hox genes at seventeen different developmental stages in *R. philippinarum*. Egg, eggs; Zyg, zygotes; Pol1, first polar body; Pol2, second polar body; C2, 2 cell; C4, 4 cell; C8, 8 cell; C16, 16 cell; C32, 32 cell; Gas, gastrula; ET, early trochophora; LT, late trochophora; Vel, veliger larvae; UL, umbo larvae; Ped, pediveliger larvae; Juv, juvenile; HC, have color juvenile.

R. philippinarum, including the chemokine receptor, D dopamine receptor, FMRFamide receptor, G-protein-coupled receptor GRL101, neuropeptide receptor, probable G-protein-coupled receptor 139, probable G-protein-coupled receptor Mth, thyrotropin-releasing hormone receptor, and cysteinyl leukotriene receptor (Table S30, Figure S15). These expanded GPCR gene families in *R. philippinarum* may participate in the regulation of various physiological functions, especially immune functions and the inflammatory response, which are potentially important for stress resistance and the clam's adaptation to benthic life.

DISCUSSION

Notably, the contig N50 of *R. philippinarum* was 28.1 kb, which is similar to those of other species in the bivalve lineage. Moreover, the complete BUSCOs in the genome of *R. philippinarum* was 92.2%, which was higher than that in *Modiolus philippinarum*, *Limnoperna fortunei*, *Argopecten purpuratus*, *C. gigas*, *O. bimaculoides*, and *Saccostrea glomerata* (Table S31 and Figure S16). In summary, the genome assembly index of *R. philippinarum* was similar to that of other species of Mollusca.

Ruditapes philippinarum has a variety of colors and a distinct set of genes that are either expanded or highly expressed and facilitate its adaptation to extreme environments. Many bivalves express multiple tyrosinases, and the expansion of the tyrosinase genes appears to be a common feature of bivalves, with more than 20 gene family members present in *R. philippinarum*, *C. gigas*, *P. fucata*, and *Patinopecten yessoensis* (Table S32). In the present study, qPCR analyses of the *Mitf* and *Tyr* genes showed that the *Tyr* genes have a

distinctive expression pattern in different developmental stages and that *Mitf* gene expression increases significantly from the early development stages that lack pigmentation to the juvenile stages with colored shells. This indicates the potential roles of these genes in shell biomineralization and shell color pigmentation. Three *Mitf* genes are uniquely expressed in the O strain, suggesting that these *Mitf* proteins are involved in the pigmentation responsible for its orange color. The distinctive expression patterns of the *Mitf* and *Tyr* genes that were demonstrated with RNA-seq and qPCR analyses shed light on the molecular basis of shell pigmentation and the color diversity in the Manila clam.

Here, we have provided an overview of the immune-related genes of the Manila clam that were identified with genomic, transcriptomic, and comparative genomic analyses. The ability of the immune system to detect pathogen-derived molecules is mediated by pattern recognition receptors (PRRs) (Janeway and Medzhitov, 2002). Several groups of invertebrate PRRs have been characterized in the Manila clam, such as TEPs, Toll-like receptors, peptidoglycan recognition proteins, fibrinogen-related proteins, galectins, C-type lectins, and complement-related proteins. In this study, the TEP superfamily genes were shown to be expanded in the *R. philippinarum* genome. TEPs bind to the surfaces of exogenous microorganisms with conserved thioester bonds, triggering a series of immune responses, including the activation of the complement system and phagocytosis (Fujita, 2002).

Complement component 3 (C3) is central to the complement system, and plays an important role in immune defense, immune regulation, and immune pathology. C3 is the core member of the complement system because it is the intersection of several activation pathways, and depends on a positive feedback loop from C3b. Upon its proteolytic activation, C3b binds covalently to the surface molecules of microbes via intrachain thioester bonds and initiates the formation of the membrane-attack complex (MAC), which eliminates invading pathogens via the lytic pathway (Anderluh and Gilbert, 2014). A C3a-like peptide has been shown to mediate the chemotaxis of hemocytes in *Ciona intestinalis* (Pinto et al., 2003) and *Pyura stolonifera* (Raftos et al., 2003). The activated fragments of C3 (C3a and C3b) are also involved in the activation of macrophages and mastocytes (Gao et al., 2013).

C3 is a gene conserved throughout evolution, from cnidarians to humans (Sahu and Lambris, 2001). The number of *C3* gene isoforms in highly evolved vertebrates is small, but there is usually a large number of *C3* genes in primitive vertebrates and invertebrates, although the number varies between species (Huan et al., 2012). C3 is an essential molecule in the complement system, acting as an opsonin in the phagocytosis of microorganisms. Therefore, as an important part of the immune system, C3 is particularly crucial to shellfish health because most shellfish lack an adaptive immune system. The number of genes in the *TEP* superfamily (C3, CD109, and A2M) is higher in the Manila clam than in other bivalve species (Table S27), suggesting that *TEP* expansion is related to the immune defense system and benthic adaptation of the Manila clam. The complement pathway genes (*SABL*, *C1qDCs*, *C3*, *C3a*, *C3b*) are also expanded in the Manila clam, which is evidence of an association between gene duplication and pathogen-rich ecological conditions. The pathogen recognition mechanisms of *R. philippinarum* include the pathogen-recognition receptors C1qDCs, Bf, and carbohydrate-binding lectins. The expansion of the *C1q* genes in the Manila clam has also been reported by Mun et al. (2017). Zhang et al. (2015) demonstrated that the *C1qDC* genes are expanded in the Pacific oyster and that C1qDC expression is upregulated by both biotic and abiotic challenges.

Transcriptomic analyses and qPCR confirmation showed that *Hsp70* expression increased significantly in *R. philippinarum* after hypoxia stress for 2 or 5 days. The expression of *Hsp70* also increased significantly after exposure to a parasite or acidification. Therefore, the *Hsp70* genes are considered to be involved in the multistress resistance of *R. philippinarum*. Hierarchical clustering showed that the *Hsp70* genes have different expression patterns at different developmental stages (Figure S11). The first cluster of eight *Hsp70* mRNAs is only expressed in the pelagic larval stages, whereas other *Hsp70* genes are mainly expressed in the pediveliger larval stages, implying that Hsp70 has potential roles in the immune responses in the different larval stages of the Manila clam. Overall, the expansion of the immune-related gene families (*HSP70*, *C3*, *SABL*, and *lysozyme*) is vital to the resistance to extreme conditions and the benthic adaptation of *R. philippinarum*.

The *Hox* gene family directs morphological development and tissue differentiation along all the principal axes of an embryo. Many *Hox* genes are expressed during early embryogenesis, suggesting their roles in

development (Krumlauf et al., 1987; Utset et al., 1987; Dolecki et al., 1988). The overall form assumed during embryonic development is controlled by the actions of the Hox proteins, their cofactors, and ultimately by the DNA regulatory elements that control their expression (Lufkin, 2005; Hejnol and Martindale, 2009; Hinman et al., 2003). In *Gibbula varia*, the strong expression of *Gva-Hox2* was observed in trochophore and D-shaped larvae, whereas *Gva-Post2* was expressed in cells around the shell field in the early trochophore, which form the future mantle edge (Samadi and Steiner, 2009). In the present study, *Post2* was strongly expressed in the trochophore, veliger, and umbo larvae, demonstrating its significant role in larval development. *Lox5* was mainly expressed in the umbo larva, suggesting that Lox5 is involved in regulating morphogenesis. In *G. varia*, the expression of *Gva-Lox5* is lost in the velum of the posttorsional veliger, although the gene is still expressed in the cerebral ganglia and their commissures (Samadi and Steiner, 2009). High levels of *Hox1* and *Hox4* expression were detected in the D-shaped larvae of both the oyster and scallop (Zhang et al., 2012; Wang et al., 2017). The Hox proteins play pivotal roles in molluscan larval development and shell formation (Lufkin, 2005).

In conclusion, the expansion of the immune-related genes and complement pathways plays an important role in the benthic adaptation of the Manila clam. The ecology of a benthic lifestyle implies that these animals interact with high concentrations of microorganisms at the low oxygen levels in sediments. However, the Manila clam has well-adapted defense strategies to protect itself from pathogens and is recognized as a robust species that is extremely resistant to adverse environmental conditions.

Limitations of the Study

Here, we have provided a comprehensive framework for understanding the genetic adaptations of *R. philippinarum* to the benthic environment. Although the quality and contiguity of the *R. philippinarum* genome assembly was carefully validated and was generally reliable for the current study, the contig/scaffold N50 did not reach the optimal level for molluscan genome assemblies. With the development of the high-throughput sequencing technology, the quality of the assembly will be improved in future studies. The asymmetry in the quality of the two clam genomes compared means that the findings from this comparison must be considered with caution. Functional experimental assays are also required to confirm the expansion of these gene families and to identify the targets involved in the adaptation of *R. philippinarum* to its hypoxic, pathogen-rich environment.

METHODS

All methods can be found in the accompanying Transparent Methods supplemental file.

SUPPLEMENTAL INFORMATION

Supplemental Information can be found online at https://doi.org/10.1016/j.isci.2019.08.049.

ACKNOWLEDGMENTS

We thank Professor Guofan Zhang (Institute of Oceanology, Chinese Academy of Sciences) for his insightful comments and constructive suggestions on this work. Many thanks are also given to Prof. Ximing Guo from Rutgers University, Prof. Li Li from Institute of Oceanology, Chinese Academy of Sciences, Prof. Kenneth M. Halanych and Dr. Yuanning Li from Auburn University for giving helpful suggestions, Prof. Kyudong Han and Seyoung Mun from Dankook University for sharing the data with us. This study was supported by the National Key R&D Program of China (2018YFD0901400), the Modern Agro-industry Technology Research System (CARS-49), Liaoning Revitalization Talents Program (XLYC1807271), Liaoning BaiQianWan Talents Program, the Scientific Research project of Liaoning Education Department (QL201703), and Dalian high-level talent innovation support program (Dalian Youth Science and Technology Star Project Support Program) (2016RQ065).

AUTHOR CONTRIBUTIONS

X.Y. and H.N. conceived the study and designed major scientific objectives. X.Y., H.N., Z.H., J.D., and M.Z. coordinated the whole project. M.Z., L.Y., L.J., Z.M., H.W., and X.M. prepared clam materials for genome and transcriptome sequencing. L.J. and H.W. conducted DNA extraction, and M.Z. prepared large-insert genomic libraries. H.N., L.Y., Z.M., and X.M. participated initial genome analysis. M.Z. and H.N. conducted genome sequencing, assembly, annotation, and gene family analysis. M.Z. conducted library preparation for genome resequencing, and G.R., L.Y., L.J., Z.M., H.W., and X.M. conducted mRNA extraction and library

preparation for transcriptome sequencing. H.N., Z.M., J.D., and L.Y. participated in genome polymorphism analysis. L.Y. and L.J. participated in shell color-related genes and pigment pathway analysis, and H.W. and C.C. participated in hypoxia transcriptome analysis. L.Y. and Z.M. participated in developmental transcriptome analysis, and H.Y. and T.H. performed ocean acidification experiments. X.M. participated in parasites transcriptome analysis. D.L. and P.C. conducted the immune response of *R. philippinarum* under different pathogenic stimuli (LPS, PGN, and Poly I:C). Z.L. provided computational services and technical support. H.N., Z.H., J.D., and Z.L. participated in final data analysis and interpretation. H.N., Z.L., and G.L. did most of the writing with input from other authors.

DECLARATION OF INTERESTS

The authors declare no competing interests.

Received: February 3, 2019
Revised: June 5, 2019
Accepted: August 27, 2019
Published: September 27, 2019

REFERENCES

G. Anderluh, and R. Gilbert, eds. (2014). MACPF/CDC Proteins - Agents of Defence, Attack and Invasion (Springer). https://doi.org/10.1007/978-94-017-8881-6.

Cerenius, L., Lee, B.L., and Söderhäll, K. (2008). The proPO-system: pros and cons for its role in invertebrate immunity. Trends Immunol. *29*, 263–271.

Choi, K.S., Park, K.I., Lee, K.W., and Matsuoka, K. (2002). Infection intensity, prevalence and histopathology of *Perkinsus* sp. in the manila clam, *Ruditapes philippinarum*, in Isahaya Bay, Japan. J. Shellfish Res. *21*, 119–125.

Daniel, B. (2013). Marine Environmental Biology and Conservation (Jones & Bartlett Learning), p. 46.

Dolecki, G.J., Wang, G., and Humphreys, T. (1988). Stage- and tissue-specific expression of two homeo box genes in sea urchin embryos and adults. Nucleic Acids Res. *16*, 11543–11558.

Dyachuk, V.A. (2016). Hematopoiesis in bivalvia larvae: cellular origin, differentiation of hemocytes, and neoplasia. Dev. Comp. Immunol. *65*, 253–257.

FAO (2017). Fisheries department publications in FAO fisheries and aquaculture department. http://www.fao.org/3/a-i7989t.pdf.

Feng, D., Li, Q., Yu, H., Zhao, X., and Kong, L. (2015). Comparative Transcriptome analysis of the pacific oyster *Crassostrea gigas* characterized by shell colors: identification of genetic bases potentially involved in pigmentation. PLoS One *10*, e0145257.

Feng, D., Li, Q., Yu, H., Kong, L., and Du, S. (2018). Transcriptional profiling of long non-coding RNAs in mantle of *Crassostrea gigas* and their association with shell pigmentation. Sci. Rep. *8*, 1436.

Findlay, R., and Battin, T. (2016). The microbial ecology of benthic environments, p 4.2.1-1-4.2.1-20. In Manual of Environmental Microbiology, Fourth Edition, M. Yates, C. Nakatsu, R. Miller, and S. Pillai, eds. (ASM Press). https://doi.org/10.1128/9781555818821.ch4.2.1.

Fujita, T. (2002). Evolution of the lectin–complement pathway and its role in innate immunity. Nat. Rev. Immunol. *2*, 346–353.

Gao, Z., Li, M., Wu, J., and Zhang, S. (2013). Interplay between invertebrate C3a with vertebrate macrophages: functional characterization of immune activities of amphioxus C3a. Fish Shellfish Immunol. *35*, 1249–1259.

Gestal, C., Roch, F., Renault, T., Pallavicini, A., Paillard, C., Novoa, B., Oubella, R., Venier, P., and Figueras, A. (2008). Study of diseases and the immune system of bivalves using molecular biology and genomics. Rev. Fish Sci. *16* (S1), 133–156.

Hejnol, A., and Martindale, M.Q. (2009). Coordinated spatial and temporal expression of Hox genes during embryogenesis in the acoel *Convolutriloba longifissura*. BMC Biol. *7*, 65.

Hinman, V.F., O'Brien, E.K., Richards, G.S., and Degnan, B.M. (2003). Expression of anterior Hox genes during larval development of the gastropod *Haliotis asinine*. Evol. Dev. *5*, 508–521.

Huan, P., Wang, H., and Liu, B. (2012). Transcriptomic analysis of the clam *Meretrix meretrix* on different larval stages. Mar. Biotechnol. *14*, 69.

Janeway, C.A., and Medzhitov, R. (2002). Innate immune recognition. Annu. Rev. Immunol. *20*, 197–216.

Ki, Y.M., Park, K.I., Choi, K.S., Alvarez, R.A., Cummings, R.D., and Cho, M. (2006). Lectin from the Manila clam *Ruditapes philippinarum* is induced upon infection with the protozoan parasite *Perkinsus olseni*. J. Biol. Chem. *281*, 26854–26864.

Kodama, K., Waku, M., Sone, R., Miyawaki, D., Ishida, T., Akatsuka, T., and Horiguchi, T. (2018). Ontogenetic and temperature-dependent changes in tolerance to hypoxia and hydrogen sulfide during the early life stages of the Manila clam *Ruditapes philippinarum*. Mar. Environ. Res. *137*, 177–187.

Krumholz, A., Yao, J., Wang, L.V., vanVickle-Chavez, S.J., Fleming, T., and Gillanders, W.E. (2011). Photoacoustic microscopy of tyrosinase reporter gene in vivo. J. Biomed. Opt. *16*, 080503.

Krumlauf, R., Holland, P.W., McVey, J.H., and Hogan, B.L. (1987). Developmental and spatial patterns of expression of the mouse homeobox gene, Hox 2.1. Development *99*, 603–617.

Lemer, S., Saulnier, D., Gueguen, Y., and Planes, S. (2015). Identification of genes associated with shell color in the black-lipped pearl oyster, *Pinctada margaritifera*. BMC Genomics *16*, 568.

Lim, H.S., Diaz, R.J., Hong, J.S., and Schaffner, L.C. (2006). Hypoxia and benthic community recovery in Korean coastal waters. Mar. Pollut. Bull. *52*, 1517–1526.

Lufkin, T. (2005). Hox Genes: Embryonic Development (eLS).

Mann, K., and Jackson, D.J. (2014). Characterization of the pigmented shell-forming proteome of the common grove snail *Cepaea nemoralis*. BMC Genomics *15*, 249.

Milan, M., Coppe, A., Reinhardt, R., Cancela, L.M., Leite, R.B., Saavedra, C., Ciofi, C., Chelazzi, G., Patarnello, T., Bortoluzzi, S., and Bargelloni, L. (2011). Transcriptome sequencing and microarray development for the Manila clam, *Ruditapes philippinarum*: genomic tools for environmental monitoring. BMC Genomics *12*, 234.

Mun, S., Kim, Y.-J., Markkandan, K., Shin, W., Oh, S., Woo, J., Yoo, J., An, H., and Han, K. (2017). The whole-genome and transcriptome of the manila clam (*Ruditapes philippinarum*). Genome Biol. Evol. *9*, 1487–1498.

Nie, H., Liu, L., Huon, Z., Chen, P., Ding, J., Yang, F., and Yan, X. (2017a). The Hsp70 gene expression responses to thermal and salinity stress in wild and cultivated Manila clam *Ruditapes philippinarum*. Aquaculture *470*, 149–156.

Nie, H., Chen, P., Huo, Z., Chen, Y., Hou, X., Yang, F., and Yan, X. (2017b). Effects of temperature and salinity on oxygen consumption and ammonia excretion in different color strains of the Manila clam, *Ruditapes philippinarum*. Aquaculture Res. *48*, 2778–2786.

Norkko, J., and Shumway, S.E. (2011). Bivalves as bioturbators and bioirrigators. In Shellfish Aquaculture and the Environment Chapter: 10, S.E. Shumway, ed. (Wiley Science Publishers), pp. 297–317.

Peignon, J.M., Gérard, A., Naciri, Y., Ledu, C., and Phélipot, P. (1995). Analysis of shell color determinism in the Manila clam *Ruditapes philippinarum*. Aquat. Living Resour. *8*, 181–189.

Pinto, M.R., Chinnici, C.M., Kimura, Y., Melillo, D., Marino, R., Spruce, L.A., De Santis, R., Parrinello, N., and Lambris, J.D. (2003). CiC3-1a-mediated chemotaxis in the deuterostome invertebrate *Ciona intestinalis* (Urochordata). J. Immunol. *171*, 5521–5528.

Pretto, T., Zambon, M., Civettini, M., Caburlotto, G., Boffo, L., Rossetti, E., and Arcangeli, G. (2014). Massive mortality in Manila clams (*Ruditapes philippinarum*) farmed in the lagoon of Venice, caused by *Perkinsus olseni*. Bull. Eur. Assoc. Fish Pathol. *34*, 43–53.

Protas, M.E., and Patel, N.H. (2008). Evolution of coloration patterns. Annu. Rev. Cell Dev. Biol. *24*, 425–446.

Raftos, D.A., Robbins, J., Newton, R.A., and Nair, S.V. (2003). A complement component C3a-like peptide stimulates chemotaxis by hemocytes from an invertebrate chordate-the tunicate, *Pyura stolonifera*. Comp. Biochem. Physiol. A *134*, 377–386.

Sahu, A., and Lambris, J.D. (2001). Structure and biology of complement protein C3, a connecting link between innate and acquired immunity. Immunol. Rev. *180*, 35.

Samadi, L., and Steiner, G. (2009). Involvement of Hox genes in shell morphogenesis in the encapsulated development of a top shell gastropod (*Gibbula varia* L.). Dev. Genes Evol. *219*, 523–530.

Shimokawa, J., Yoshinaga, T., and Ogawa, K. (2010). Experimental evaluation of the pathogenicity of Perkinsus olseni in juvenile Manila clams *Ruditapes philippinarum*. J. Invertebr. Pathol. *105*, 347–351.

Simakov, O., Marletaz, F., Cho, S.J., Edsinger-Gonzales, E., Havlak, P., Hellsten, U., Kuo, D.H., Larsson, T., Lv, J., Arendt, D., Savage, R., et al. (2013). Insights into bilaterial evolution from three spiralian genomes. Nature *493*, 526–531.

Song, L., Wang, L., Qiu, L., and Zhan, H. (2010). Bivalve immunity. In Invertebrate Immunity. Advances in Experimental Medicine and Biology, *708*, K. Söderhäll, ed. (Springer), pp. 44–65.

Steckbauer, A., Ramajo, L., Ramajo, L., Hendriks, I.E., Fernandez, M., Lagos, N.A., Prado, L., and Duarte, C.M. (2015). Synergistic effects of hypoxia and increasing CO2 on benthic invertebrates of the central Chilean coast. Front. Mar. Sci. *2*, 1–12.

Sun, X., Yang, A., Wu, B., Zhou, L., and Liu, Z. (2015). Characterization of the mantle transcriptome of Yesso scallop (*Patinopecten yessoensis*): identification of genes potentially involved in biomineralization and pigmentation. PLoS One *10*, e0122967.

Takeuchi, T., Kawashima, T., Koyanagi, R., Gyoja, F., Tanaka, M., Ikuta, T., Shoguchi, E., Fujiwara, M., Shinzato, C., Hisata, K., et al. (2012). Draft genome of the pearl oyster *Pinctada fucata*: a platform for understanding bivalve biology. DNA Res. *19*, 117–130.

Tamai, K. (1993). Tolerance of *Theora fragilis* (Bivalvia: Semelidae) to low concentrations of dissolved oxygen. Nippon Suisan Gakkaishi *59*, 615–620.

Utset, M.F., Awgulewitsch, A., Ruddle, F.H., and McGinnis, W. (1987). Region-specific expression of two mouse homeobox genes. Science *235*, 1379–1382.

Vaughn, C.C., and Hakenkamp, C.C. (2001). The functional role of burrowing bivalves in freshwater ecosystems. Freshw. Biol. *46*, 1431–1446.

Wang, Y., Sheng, H., He, Y., Wu, J., Jiang, Y., Tam, N.F., and Zhou, H. (2012). Comparison of the levels of bacterial diversity in freshwater, intertidal wetland, and marine sediments by using millions of illumina tags. Appl. Environ. Microbiol. *78*, 8264–8271.

Wang, S., Zhang, J., Jiao, W., Li, J., Xun, X., Sun, Y., Guo, X., Huan, P., Dong, B., Zhang, L., et al. (2017). Scallop genome provides insights into evolution of bilaterian karyotype and development. Nat. Ecol. Evol. *1*, 120.

Yue, X., Nie, Q., Xiao, G., and Liu, B. (2015). Transcriptome analysis of shell color-related genes in the clam *Meretrix meretrix*. Mar. Biotechnol. *17*, 1–11.

Zhang, G.F., and Yan, X.W. (2010). In Clam Aquaculture (Science Press), in chinese.

Zhang, G.F., Fang, X., Guo, X., Li, L., Luo, R., Xu, F., Yang, P., Zhang, L., Wang, X., Qi, H., et al. (2012). The oyster genome reveals stress adaptation and complexity of shell formation. Nature *490*, 49–54.

Zhang, L.L., Li, L., Guo, X., Litman, G.W., Dishaw, L.J., and Zhang, G. (2015). Massive expansion and functional divergence of innate immune genes in a protostome. Sci. Rep. *5*, 8693.

Zhao, L., Yang, F., Milano, S., Han, T., Walliser, E.O., and Schöne, B.R. (2018). Transgenerational acclimation to seawater acidification in the Manila clam *Ruditapes philippinarum*: preferential uptake of metabolic carbon. Sci. Total Environ. *627*, 95–103.

ISCI, Volume *19*

Supplemental Information

Clam Genome Sequence Clarifies the Molecular Basis of Its Benthic Adaptation and Extraordinary Shell Color Diversity

Xiwu Yan, Hongtao Nie, Zhongming Huo, Jianfeng Ding, Zhenzhen Li, Lulu Yan, Liwen Jiang, Zhengqiang Mu, Huamin Wang, Xiangyu Meng, Peng Chen, Mengyan Zhou, Md. Golam Rbbani, Guangjian Liu, and Dongdong Li

Fig. S1 The shell color and appearance of different strains of *R. philippinarum*. **A** Zebra strain. **B** White strain. **C** White Zebra strain. **D** Orange strain, Related to Figure 2.

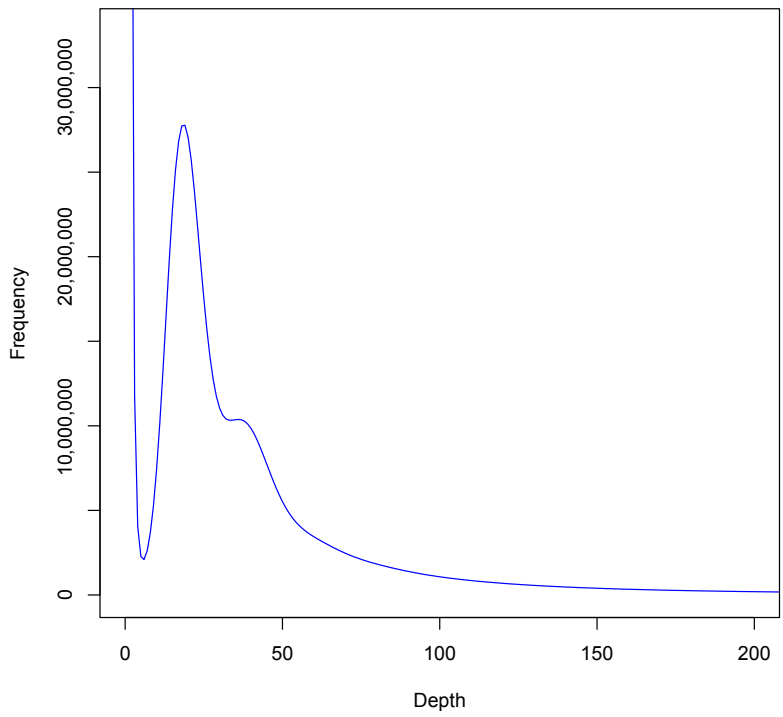

Fig. S2 Distribution of 17-mer frequency in Manila clam genome. The horizontal axis represents the K-mer depth, namely the number of times occurred. The volume of K-mer is plotted against the frequency at which they occur. The left-hand peak at low frequency and high volume represented K-mer containing essentially random sequencing errors. The main volume peak of K-mer was 38, and there was a hybrid peak at about half of the main volume peak of K-mer depth (~20 X). The genome size was estimated as 1.32 Gb by the formula 'Genome size=total_kmer_num/kmer_depth', Related to Figure 1.

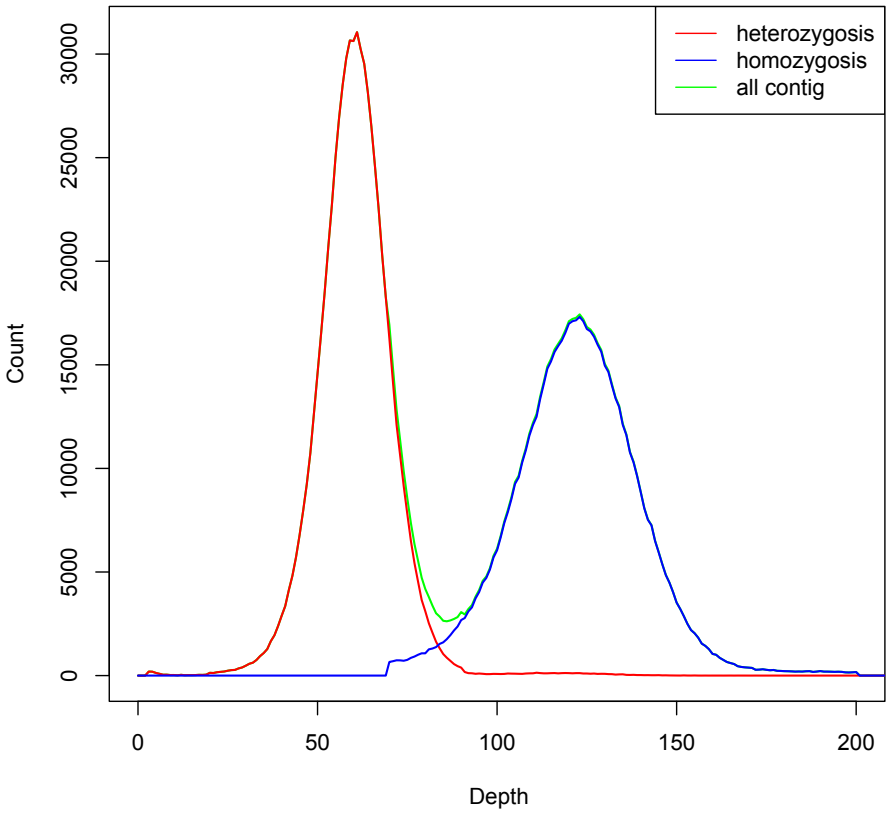

Fig. S3 The sequencing depth distribution. All high-quality reads generated from short insert size libraries were mapped onto the assembled genome, the sequencing depth of all contigs in the genome (green), contig from heterozygous regions (red) and contig from homozygous regions (blue) were plotted. The peak of contigs from homozygous contigs was 123 X, and from the heterozygous contigs was 61 X, Related to Figure 1.

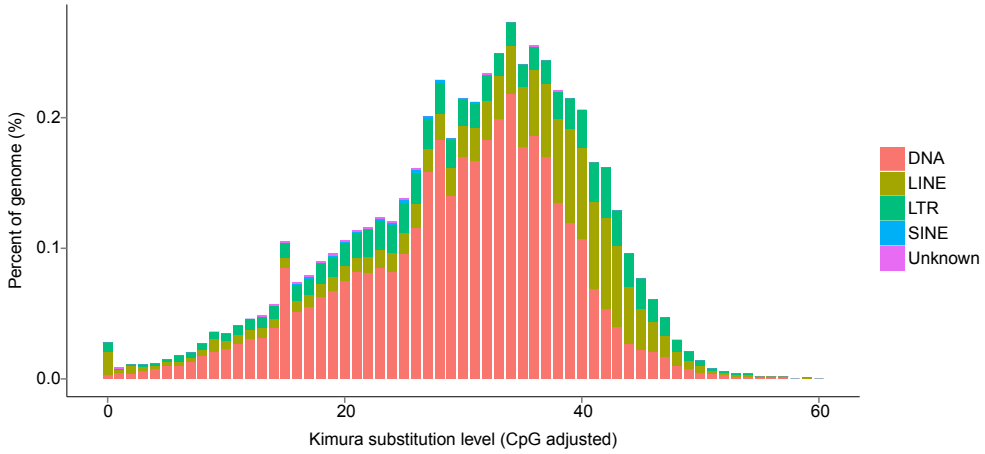

Fig. S4 Divergence distribution of classified families of TEs. Red indicated DNA transposons (DNA), dark yellow indicated long interspersed nuclear element (LINE), green indicated long terminal repeat (LTR), light blue indicated short interspersed nuclear element (SINE), and purple indicated unknown TEs, Related to Figure 1.

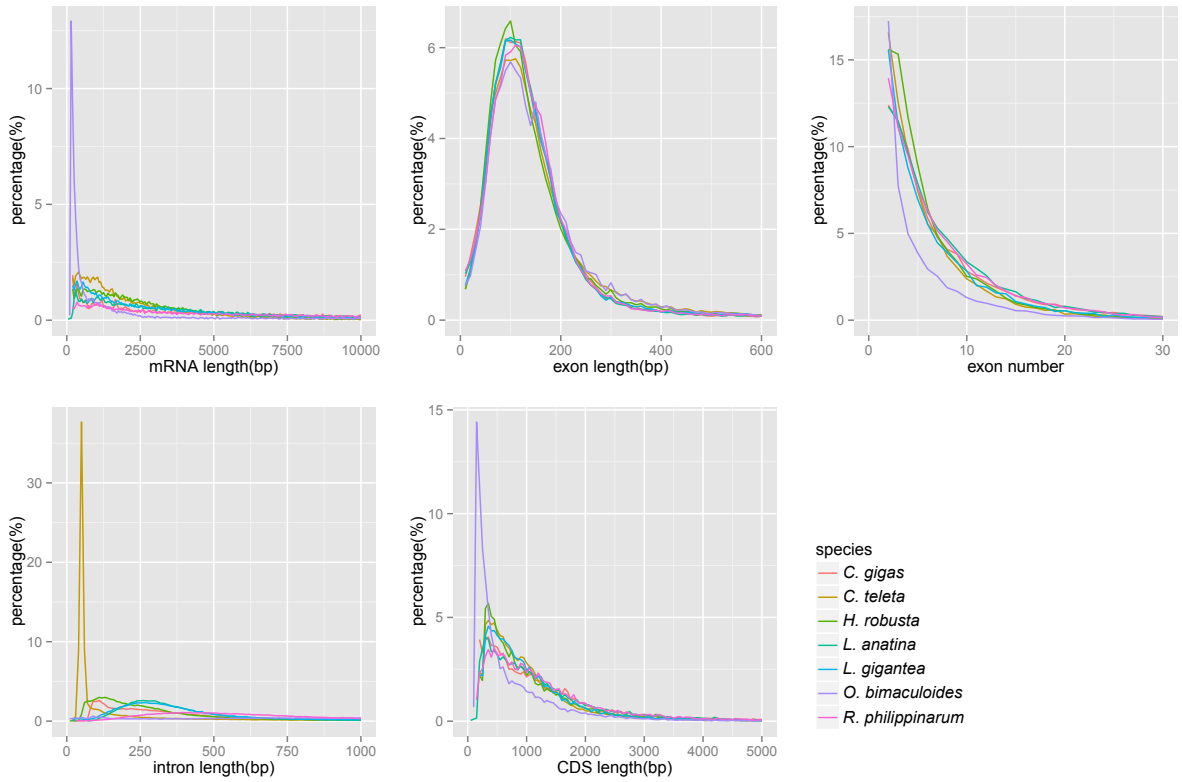

Fig. S5 Comparison of gene parameters among *R. philippinarum* genome and other Lophotrochozoa genomes. The similar gene parameters among *R. philippinarum*, *C. gigas*, *C. teleta*, *H. robusta*, *L. anatina*, *L. gigantea* and *O. bimaculoides* indicate the high quality gene structure annotation in *R. philippinarum* genome, Related to Figure 1.

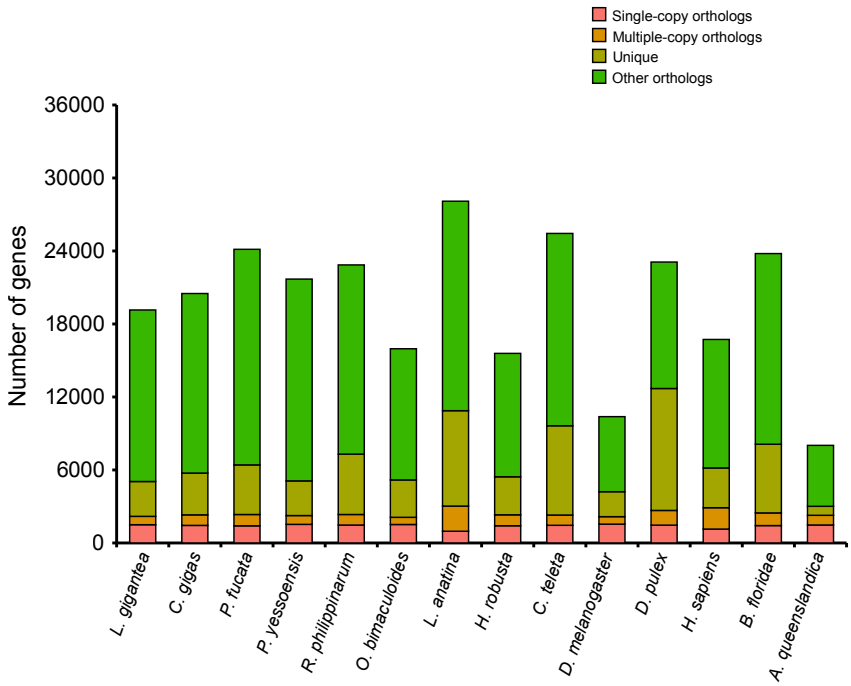

Fig. S6 The distribution of genes in different species. Pink indicated single-copy orthologs, yellow indicated multiple-copy orthologs, dark yellow indicated unique genes, and green indicated other orthologs, Related to Figure 1.

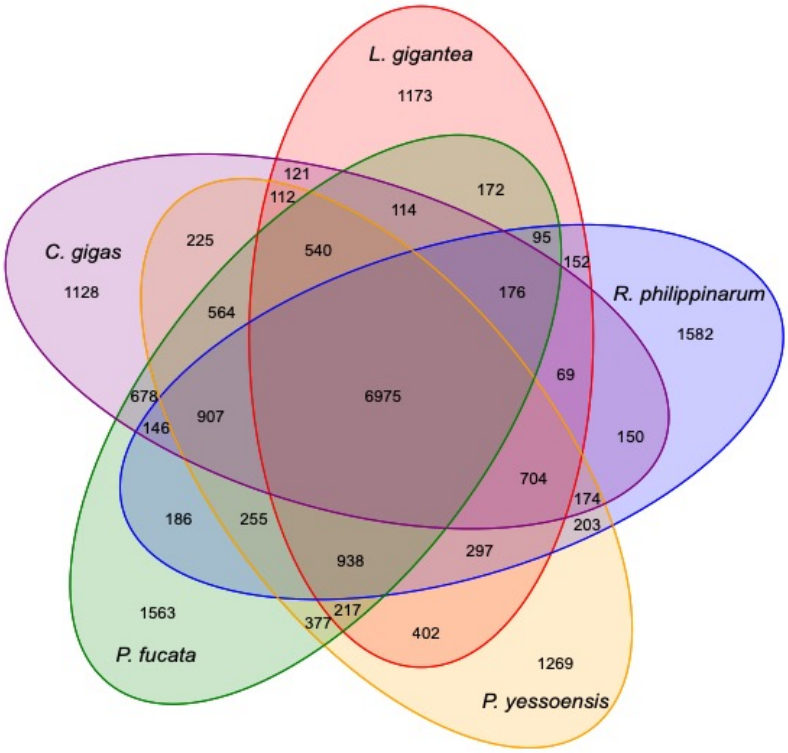

Fig. S7 The venn diagram showed common and unique gene families among five Mollusca species (*R. philippinarum*, *L. gigantea*, *C. gigas*, *P. fucata* and *P. yessoensis*). Compared with other four Mollusca species, *R. philippinarum* owned 1,582 unique gene families and shared 6,975 gene families with others, Related to Figure 1.

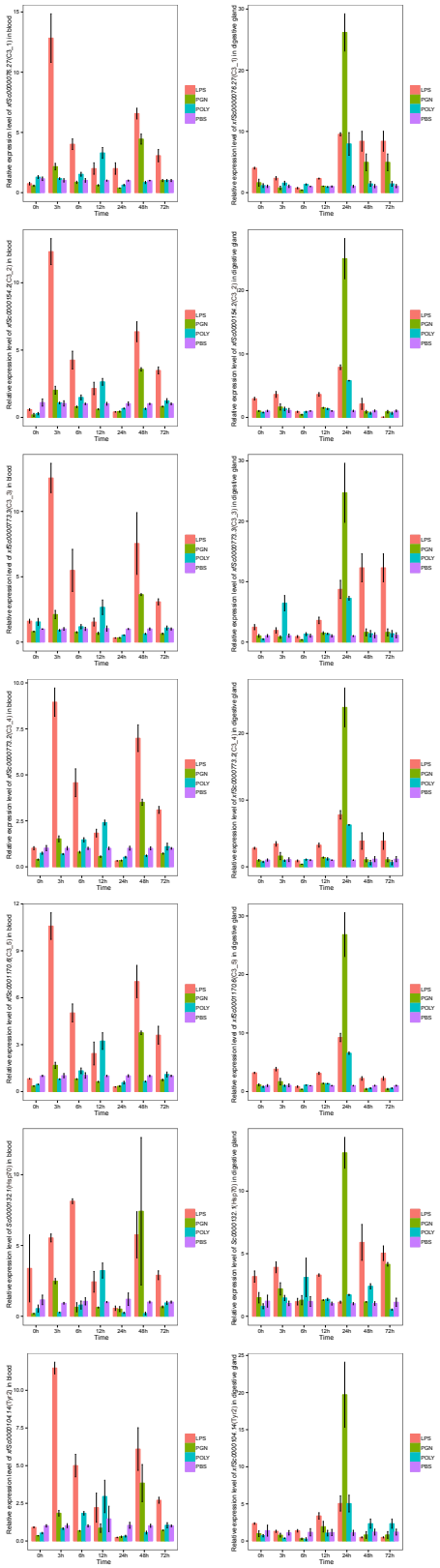

Fig. S8 The expression of key genes under different stimuli (LPS, PGN and Poly I:C), hypoxia, acidification and parasites. RT-qPCR expression of genes at 3, 6, 12, 24, 48, 72 and 96 h after the treatment of lipopolysaccharide (LPS), peptidoglycan (PGN), and polyinosinic polycytidylic acid (Poly I:C) , Related to Figure 3.

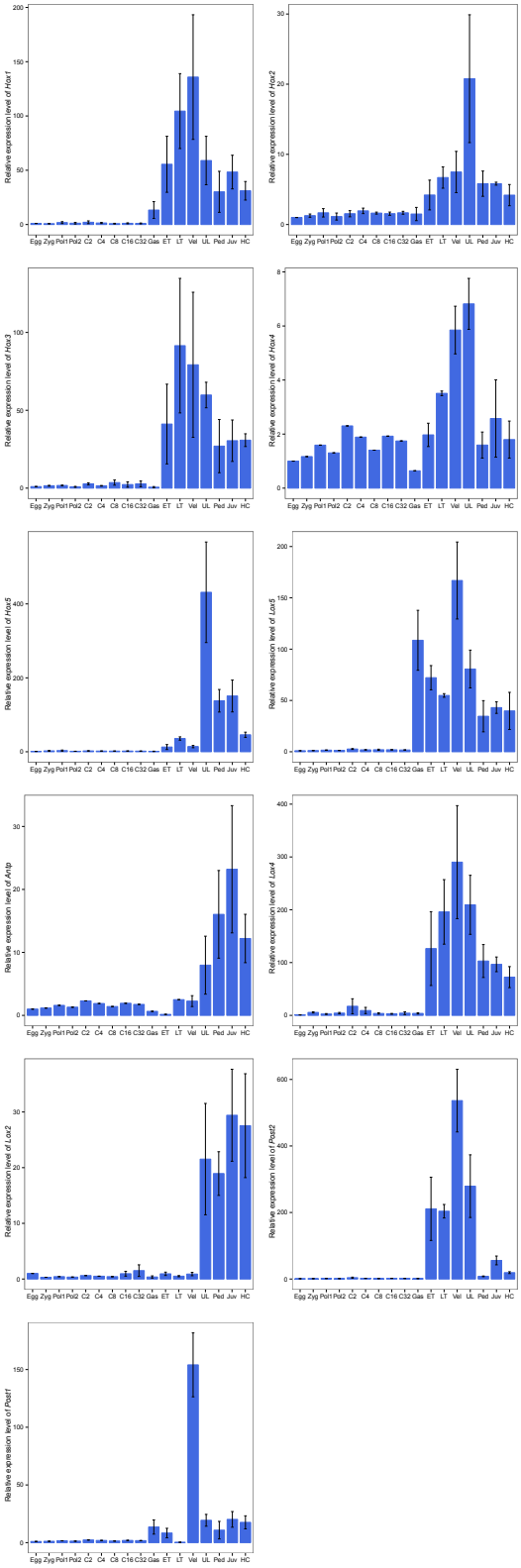

Fig. S9 RT-qPCR expression of eleven Hox genes at seventeen different developmental stages (Egg: eggs; Zyg: zygotes; Pol1: first polar body; Pol2: second polar body; C2: 2 cell; C4: 4 cell; C8: 8 cell; C16: 16 cell; C32: 32 cell; Gas: gastrula; ET: early trochophora; LT: late trochophora; Vel: veligar larvae; UL: umbo larvae; Ped: pediveliger larvae; Juv: juvenile; HC: have color juvenile) , Related to Figure 5.

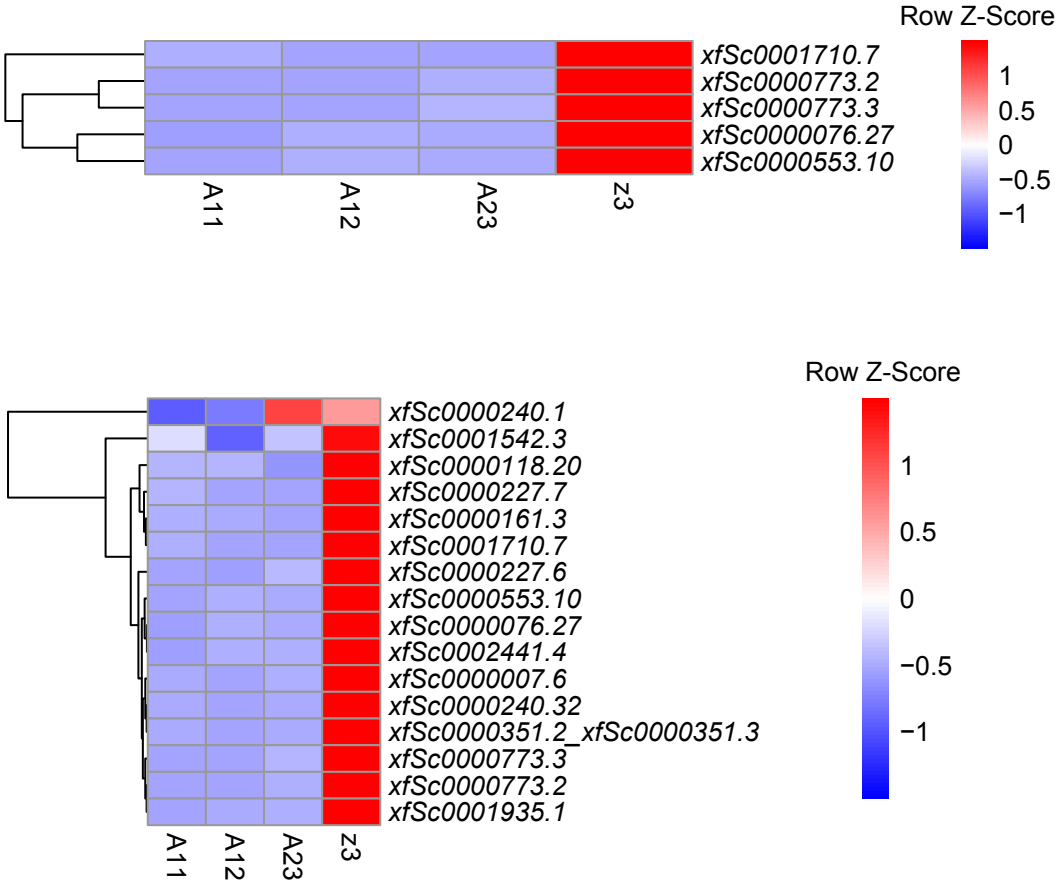

Fig. S10 RT-qPCR expression of TEP and C3 genes, Related to Figure 3.

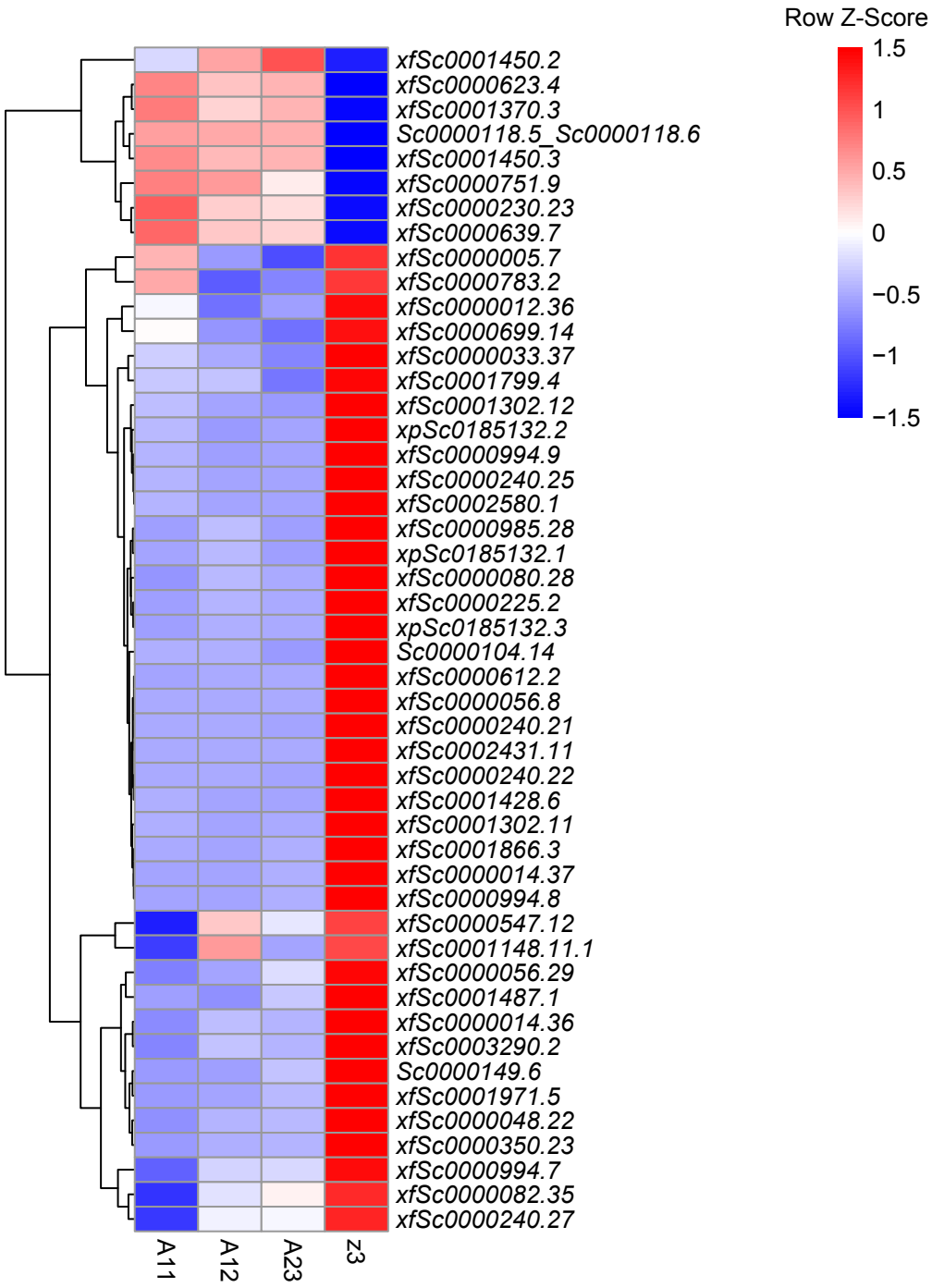

Fig. S11 Heat map and hierarchical clustering showing expression of Hsp70 genes at different developmental stages, Related to Figure 3.

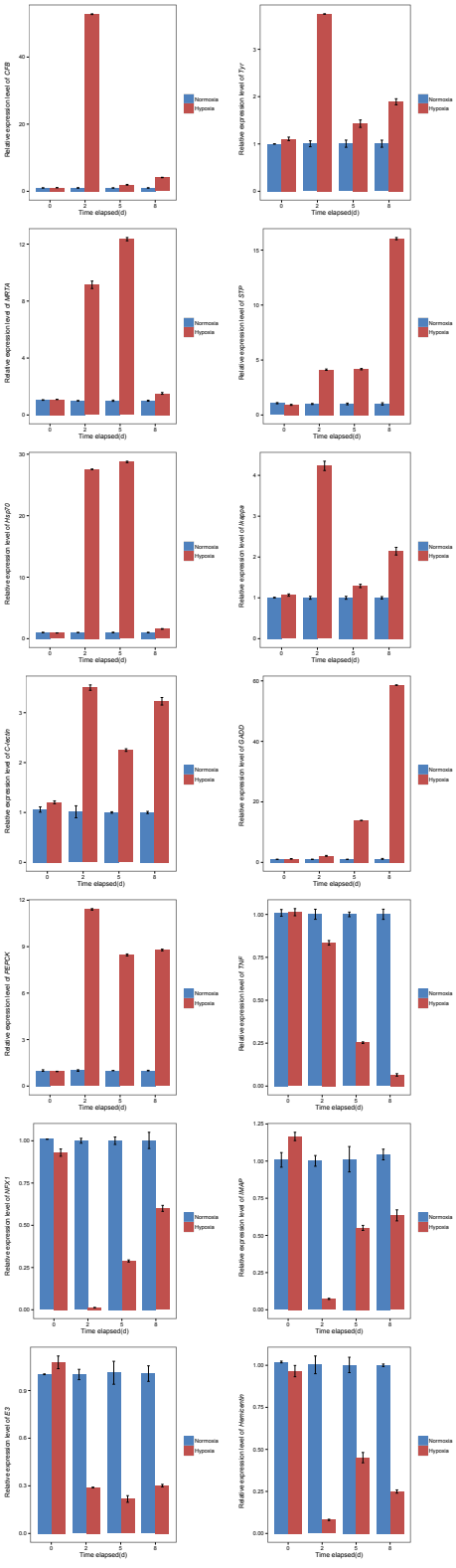

Fig. S12 RT-qPCR expression of genes at 0, 2, 5 and 8 d of hypoxia exposure, Related to Figure 3.

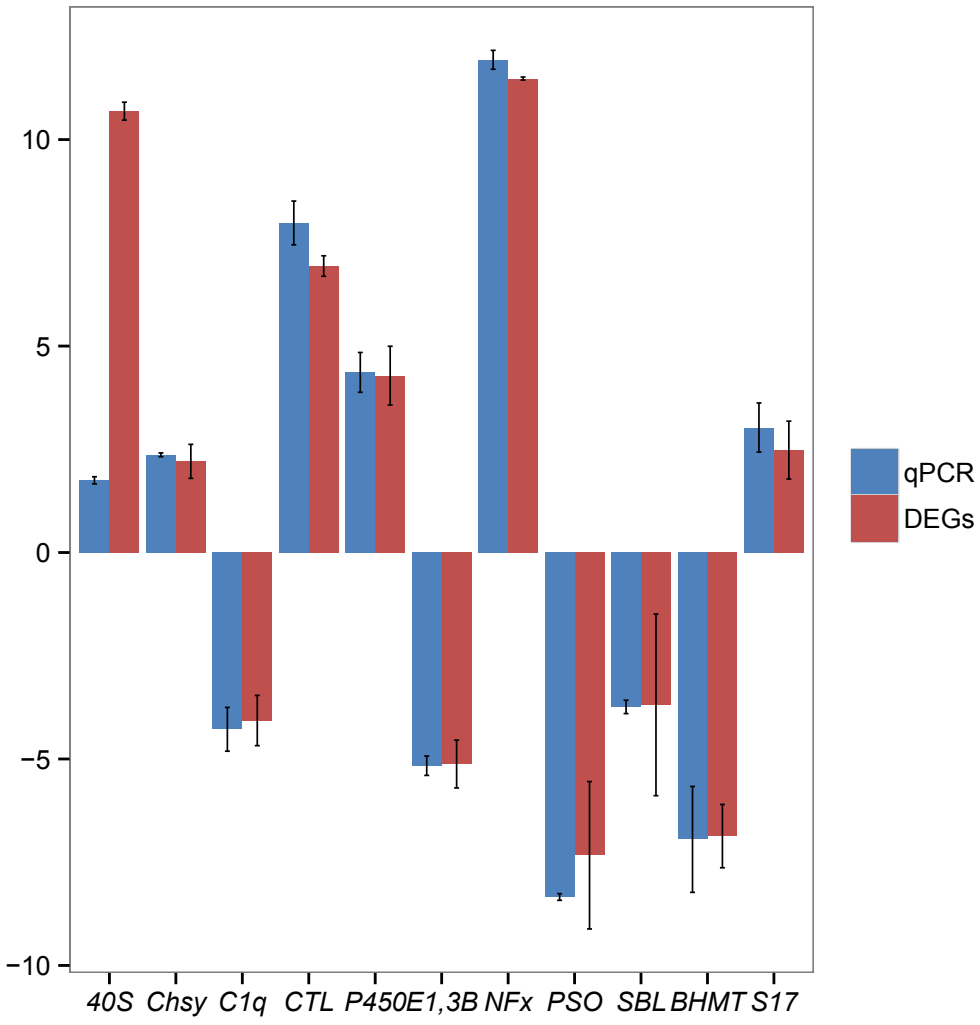

Fig. S13 RT-qPCR and DEGs expression of genes in acidification stress, Related to Figure 3.

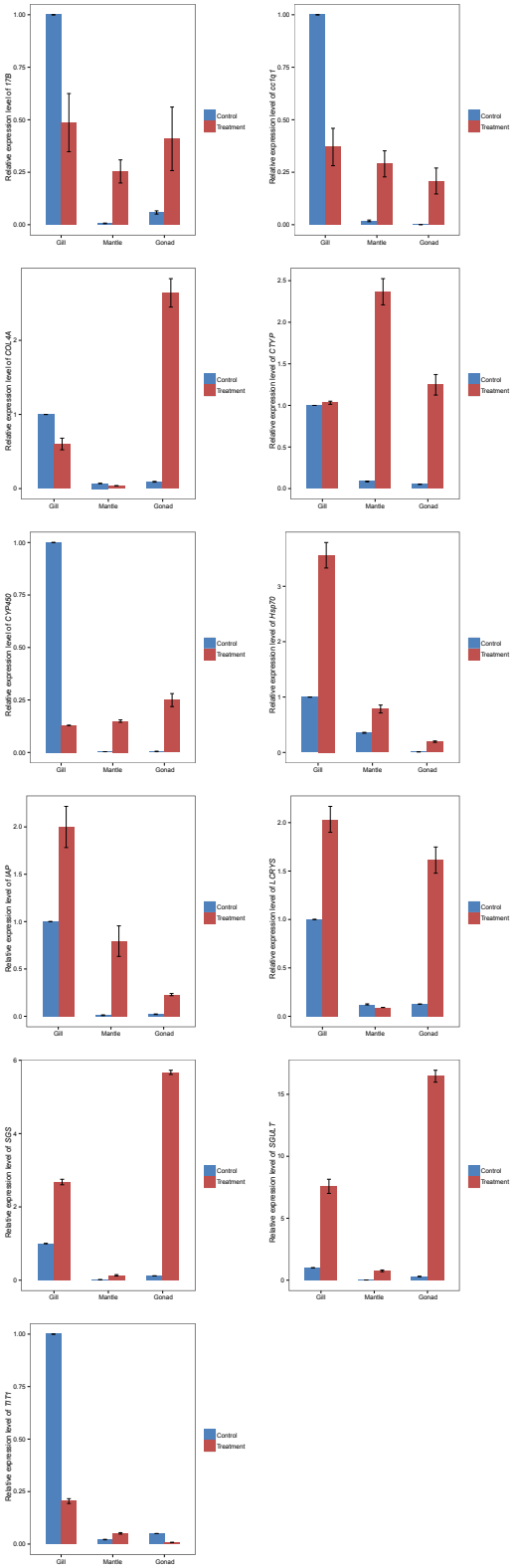

Fig. S14 RT-qPCR expression of genes in gills, mantle and gonad exposed to digenetic trematode, Related to Figure 3.

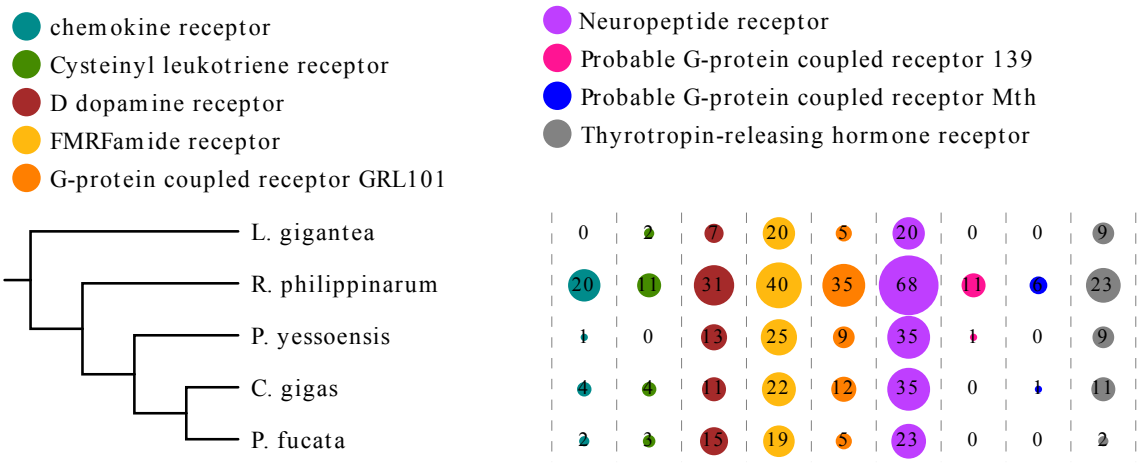

Fig. S15 The expanded function statistics of GPCR in *R. philippinarum* compared with *P. yessoensis*, *C. gigas*, *P. fucata* and *L. gigantea*, Related to Figure 4.

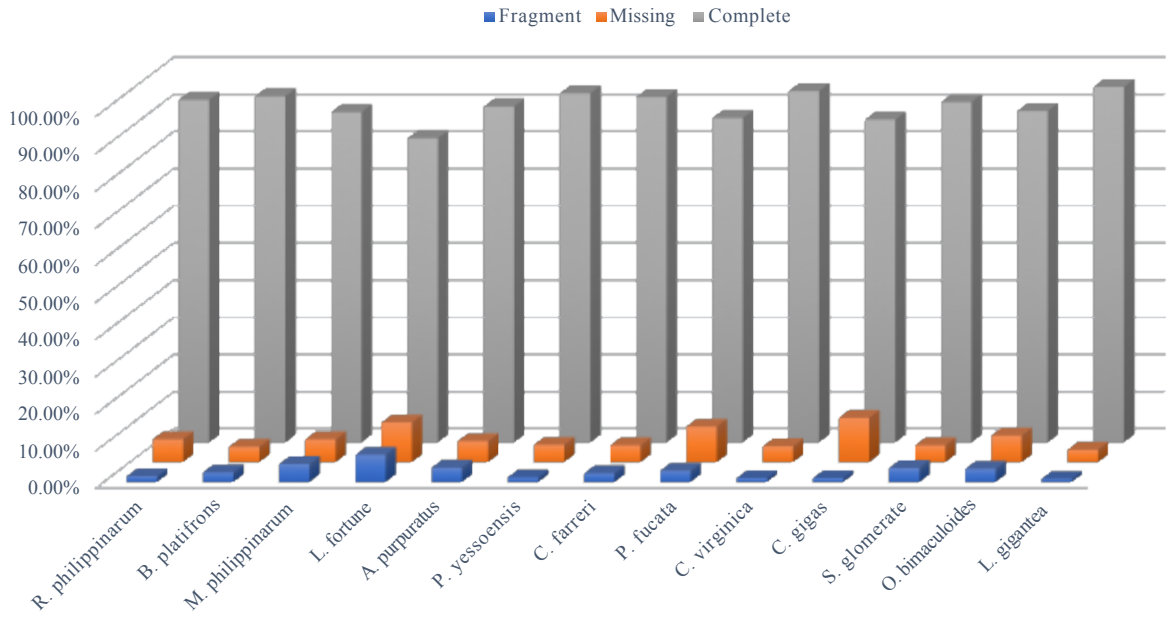

Fig. S16 The statistics of genomes of *R. philippinarum* and other homologous species. C, complete BUSCOs; F, fragmented (partial) BUSCOs; M, missing BUSCO, Related to Figure 1.

Transparent Methods

Sampling

The fifth generation of orange shell color strains of *R. philippinarum* was collected from the Zhangzidao aquaculture farm in Dalian, Liaoning Province, China. The clams with a similar shell length averaging at 20.90±1.34 mm, respectively, were used in this study. After being transported from the field to the laboratory, the clams were acclimated in aerated 70 L plastic tanks, containing water at 20 ℃ with salinity of 30. All the samples were acclimated in the laboratory for one week before the sampling. The Manila clam is not an endangered or protected species, so no specific permits were required for the study. One of the clams was sacrificed for DNA extraction.

The present study was approved by College of Fisheries and Life Science, Dalian Ocean University. Two adult individuals of orange strain of Manila clam *Ruditapes philippinarum* were selected for whole genome sequencing and genomic DNA was extracted from the whole individuals for short and long libraries of the whole-genome shotgun sequencing. One of the F6 Orange strains of Manila clam with distinctive orange shell color and highly inbred individual was selected for whole genome sequence (Fig. S1D).

Genome sequencing

Genomic DNA was broken into random fragments according to the whole genome shotgun sequencing strategy. Illumina paired-end (PE) libraries were constructed with insert size ranging from 230 bp to 500 bp. Illumina mate-pair (MP) libraries were constructed targeting insert size of 2 Kbp, 5 Kbp, 10 Kbp and 20 Kbp (35 lanes, Table S2). All the libraries were sequenced by Illumina Hiseq 2500 platform. Totally 286.1 Gb raw data was produced by PE libraries, and 135.1 Gb raw data produced by MP libraries.

To reduce the effect of sequencing error to the assembly, the following type of reads would be filtered: reads with ≥10% unidentified nucleotides for libraries, reads from short-insert libraries having more than 50% bases with quality score less than 5, reads having the sequencing adapters, read1 and read2 of two paired-end reads that were completely identical (considered to be products of PCR duplication). After filtering out the adapter sequences, low quality and duplicated reads, a total of 361.4 Gb (~274-fold coverage) data were remained as clean data for the whole-genome assembly.

To characterize the distribution of single-nucleotide polymorphism (SNP) and estimate the level of heterozygosity in the *R. philippinarum* genome, short pair-ended reads from the inbred and wild samples were aligned to the assembled genome. We identified 33,830,021 and 11,758,346 heterozygous SNPs in the assembled (inbred) and resequenced (wild) genome with the polymorphism rate of 1.038% and 1.690%, respectively (Table S4). As expected, inbreeding has significantly reduced its polymorphisms. The level of polymorphism in *R. philippinarum* is similar to that in Lingula genome (1.6%), but higher than that found in the scallop Patinopecten yessoensis (1.04%) and the Pacific oyster Crassostrea gigas (1.30%), indicating that the *R. philippinarum* genome exhibits comparatively high heterozygosity.

Estimation of genome size

The distribution of K-mer frequency is widely used for the estimation of genome size. Total of 58 Gb high-quality short-insert reads (230 bp) were used to estimate the Manila clam genome size by analyzing the K-mer frequency (defined as 17 bp here), the coverage sequencing depth of which follows Poisson distribution (Li et al., 2010). The formula 'Genome size = total_kmer_num/kmer_depth' (Liu et al., 2013), where total_kmer_num is the total number of K-mer and kmer_depth is the peak sequencing depth on the K-mer frequency distribution map, was used to estimate the genome size (Fig. S2). And the genome size of *R. philippinarum* were determined to be 1.32 Gb with high ratio of heterozygosity (Table S1).

Genome assembly

It is a challenging task to obtain a high-quality genome of R. philippinarum due to the high levels of heterozygosity (~2.0%). To tackle this challenge, an innovation assembly software NOVOheter2.0, developed by Novogene Bioinformatics Institute (Beijing, China) on basis of SOAPdenovo package (Li et al., 2010), was applied for the Manila clam genome assembly. Firstly, the heterozygous K-mers were determined from coverage information obtained from de Bruijn graph in R. philippinarum genome. All high-quality reads from short-insert size libraries were used to split and counted to generate 19-mer frequency distribution, and 19-mers with sequencing depth ranged from 23 to 124 were regarded as the initial heterozygous 19-mer set. Next, a de Bruijn graph was constructed by splitting the high-quality reads from short-insert size libraries into 45-mers with SOAPdenovo setting parameters as '-e 1 -M 1 -R', and contigs with sequencing

depth ranged from 20 to 90 were regarded as heterozygous contigs (Fig. S3).

Secondly, PE and MP reads were mapped to the heterozygous K-mer set to obtain the coverage relationship, and an effective link between two heterozygous contigs was defined if there were at least three read pairs mapped. Two contigs in a bubble represents two potential haploids in a diploid genome. The heterozygous contigs were clustered together as bubble contigs considering the order and distance between two heterozygous contigs. After clustering and classifying heterozygous contigs, there were two big groups of bubble contigs waiting to be removed in the next step.

The heterozygous contigs were matched back to the corresponding edges in de Bruijn graph constructed by 45-mers, one of the heterozygous contig groups on the edges were removed to solve the bubble structures or intricate structures in the graph caused by heterozygosity of diploid R. philippinarum genome. After merging bubble contigs, the contig sequences were obtained finally.

After obtaining contig sequences, all high-quality short-insert PE reads and large-insert MP reads were realigned onto these contigs by Platanus assembler (v1.2.1) (Kajitani et al., 2014) with scaffold protocol (default parameters). And the shared paired-end relationships between each pair of adjacent contigs were used to construct scaffolds.

Gaps in the constructed scaffolds were filled by GapCloser (English et al., 2012) (http://sourceforge.net/projects/soapdenovo2/files/GapCloser) with parameters setting as '-l 150 -p 30' based on the paired-end information of the read pairs that had one end mapped to the unique contig and the others located in the gap region.

After removing the heterozygosity in R. philippinarum genome by HaploMerger (Huang et al., 2012) with default parameters, a total of 30,811 scaffolds were assembled covering total length over 1,123 Mb. And a scaffold N50 length of 345,005 bp, contig N50 length of 28,111 bp and total length of 1.12 Gb were gained in the final Manila clam genome assembly (Table S3).

Genome evaluation

The high-quality short insert PE reads were aligned onto the assembled genome to evaluate the accuracy by using BWA (Li and Durbin, 2009) (http://bio-bwa.sourceforge.net/) with parameters setting as ‘-o 1 -i 15’. The distribution of the sequencing depth at each position was calculated to

measure the completeness of the genome assembly. The assembly with GC content equal to 31.89% (Table S5) was evaluated through mapping reads with approximately 93.32% of mapping rate and 99.83% of coverage (Table S6), explaining the completeness of the genome assembly.

Raw data of transcriptomes from the adductor muscle (5.84 Gb) were sequenced by Illumina sequencing platform. Transcripts were assembled by Trinity (Grabherr et al., 2011) with parameters setting as '-ss 0.5 -jc 0 -minkmercov 2 -minglue 2' to be as expressed sequence tags (ESTs). The 78,505 random ESTs were aligned to the scaffolds by Blat (Kent, 2002) (http://genome.ucsc.edu/goldenpath/help/blatSpec.html) with default parameters, 81.52% of which (> 200 bp) were more than 90% covered by a scaffold (Table S7). The final assembly version covered almost of the genome and the region of coding genes.

CEGMA (Parra et al., 2007) (Core Eukaryotic Genes Mapping Approach, http://korflab.ucdavis.edu/dataseda/cegma/) defined a set of conserved protein families that occur in a wide range of eukaryotes, and present a mapping procedure that accurately identifies their exon-intron structures in a novel genomic sequence. Through mapping to the 248 ultra conserved eukaryotic genes, a total of 233 genes with a ratio of 93.95% were found (Table S8), supporting a high ratio of core conserved gene families, which indicated that our assembly reached a better integrity of the core genes.

BUSCO sets (Simao et al, 2015) (Benchmarking Universal Single-Copy Orthologs: http://busco.ezlab.org/) were used to assess completeness of genome assembly combining with TBLASTN (Altschul et al, 1997), Augustus (Stanke and Waack, 2003; Stanke et al., 2006) (version 3.0.2) and HMMER (Mistry et al., 2013) (version 3.1b2). Analysis of BUSCO showed that the assembly contains 90.39% complete and 5.93% fragmented metazoa BUSCO orthologues, which suggested that the assembly is of high quality. (Table S9)

Annotation of repeats

After the genome assembly, repeat annotation was carried out for the *R. philippinarum* genome. Repetitive sequences include transposable elements (TEs) and tandem repeats. Two approaches were used to discover TEs. RepeatMasker (Smit, Chen, 2004) (version 3.3.0) found TEs in a integrate repeat library which was derived from known repeat library (Repbase 15.02) and the de novo repeat library, built by RepeatModeler (Smit, 2017) (Vision 1.0.5), RepeatScout (Price et al,

2005), and LTR_FINDER (Xu and Wang, 2007). RepeatProteinMask (Chen, 2004) was performed to detect TEs in *R. philippinarum* genome by comparing the TE protein database. Tandem repeats were ascertained in the genome using Tandem Repeats Finder (Benson, 1999). Repetitive sequences comprised ~38.30% of the *R. philippinarum* genome, and the results were shown in detail in Table S10, Table S11 and Fig. S4.

Annotation of protein coding genes

De novo predictions, homolog-based predictions and RNA-seq based predictions were employed to annotate the protein coding genes in *R. philippinarum* genome. Five ab initio gene prediction programs were used to predict genes, including Augustus (Stanke and Waack, 2003; Stanke et al., 2006) (version 3.0.2), Genescan (Salamov and Solovyev, 2000) (version 1.0), Geneid (Parra et al., 2000), GlimmerHMM (Majoros et al., 2004) (version 3.0.2) and SNAP (Korf, 2004). Protein sequences of ten homologous species (Anopheles gambiae, Caenorhabditis elegans, Crassostrea gigas, Capitella teleta, Drosophila melanogaster, Helobdella robusta, Lingula anatina, Lottia gigantea, Octopus bimaculoides, Strongylocentrotus purpuratus) were downloaded from Ensembl or NCBI. Homologous sequences were aligned against to the repeat-masked *R. philippinarum* genome using TBLASTN (Altschul et al., 1997) (E-value $\leqslant$ 1E-05). Genewise (Birney et al., 2004) (version 2.2.0) was employed to predict gene models based on the alignment sequences. There were two ways to assemble the RNA-seq data into the unique sequences of transcripts. One was mapping the RNA-seq data to the *R. philippinarum* genome using Tophat (Trapnell et al., 2009) (version 2.0.8) and using cufflinks (Trapnell et al., 2010) (version 2.1.1) (http://cufflinks.cbcb.umd.edu/) for transcript assembly. The other was applying Trinity (Grabherr et al, 2011) to assemble the RNA-seq data, and then PASA (Haas et al., 2003) software (http://pasapipeline.github.io/) improved the gene structures. A weighted and non-redundant gene set was generated by EVidenceModeler (EVM) (Haas et al., 2008) which merged all genes models predicted by the above three approaches. Combining with transcript assembly, PASA adjusted the gene models generated by EVM. At last, the gene set were filtered according to the following standards: coding region lengths of $\leqslant$ 50 amino acids, supported only by de novo methods and with FPKM < 5. The final reference gene set contained 27,652 protein coding genes. (Table S12, Table S13 and Fig. S5)

Functional annotation

Functional annotation of protein coding genes was obtained according to best BLAST hit by BLASTP (E-value ≤ 1E-05) against SwissProt (Bairoch and Apweiler, 2000), TrEMBL (Bairoch and Apweiler, 2000) and NCBI non-redundant (NR) protein databases. Motifs and domains were annotated by using InterProScan (Mulder and Apweiler, 2007) (version 4.7) to search against InterPro (Mulder and Apweiler, 2007) (v29.0) databases, including Pfam, PRINTS, PROSITE, ProDom and SMART. A Gene Ontology (Ashburner et al., 2000) (GO) term for each gene were achieved from the corresponding InterPro descriptions. Additionally, gene set was mapped to a KEGG (Kanehisa and Goto, 2000) pathway to identify the best match classification for each gene. Finally, 24,570 protein coding genes (accounting for 88.85%) owned functional annotation. (Table S14)

Non-coding RNA annotation

The tRNA genes were predicted by tRNAscan-SE software (Lowe and Eddy, 1997). The miRNA and snRNA fragments were identified by INFERNAL (Nawrocki et al, 2009) software against the Rfam (Griffiths-Jones et al., 2005) database. The rRNA were found by using BLASTN (E-value ≤1E-10) against invertebrate rRNA database. (Table S15)

Gene family cluster

Gene families were generated by OrthoMCL (Li et al., 2003) (http://orthomcl.org/orthomcl/). First, nucleotide and protein data of 13 species (Amphimedon queenslandica, Branchiostoma floridae, Capitella teleta, Crassostrea gigas, Daphnia pulex, Drosophila melanogaster, Helobdella robusta, Homo sapiens, Lingula anatina, Lottia gigantea, Octopus bimaculoides, Patinopecten yessoensis, Pinctada fucata) were downloaded from Ensembl (Release 70), NCBI and http://marinegenomics.oist.jp/gallery/. Before an "all against all" BLASTP (E-value ≤ 1E-07) program, the longest transcript was selected from alternative splicing transcripts belonging to one gene and genes with ≤ 50 amino acids were removed. The alignments with high-scoring segment pairs (Hsps) were conjoined for each gene pair by solar (Yu et al., 2006). To identify homologous gene-pairs, more than 30% coverage of the aligned regions in both homologous genes was required. Finally, the alignments were clustered into gene families using OrthoMCL with 1.5

inflation index. After clustering, 33,076 gene families and 288 single-copy orthologs were detected across *R. philippinarum* and 13 other species (Fig. S6 and Fig. S7). GO enrichment and KEGG enrichment of unique gene families in *R. philippinarum* were presented in Table S16 and Table S17.

Phylogenetic tree construction and divergence time estimation

The above mentioned 288 shared single-copy orthologs were utilized to construct the phylogenetic tree. Protein sequences of these orthologs were aligned by MUSCLE (Edgar, 2004), then protein alignments were transformed to CDS alignments. Using this CDS alignments, the phylogenetic tree was constructed by the ML (maximum likelihood) TREE algorithm in RAxML software (Stamatakis, 2006; Stamatakis et al., 2008) (version 7.2.3). Then mcmctree program of PAML (Yang, 2007) (http://abacus.gene.ucl.ac.uk/software/paml.html) was applied to estimate divergence time among 14 species with main parameters burn-in=100,000, sample-number=100,000, and sample-frequency=2. Four calibration points were selected from Simakov et al., (2015) and TimeTree (Hedges et al., 2015) website (http://www.timetree.org) as normal priors to restrain the age of the nodes, such as 518~581 Mya for TMRCA of H.sapiens-B.floridae; 500~550Mya for TMRCA of C.gigas-L.gigantea; 305~581Mya for TMRCA of C.teleta-H.robusta; 510~543Mya for TMRCA of D.pulex-D.melanogaster. The phylogenetic tree confirmed the grouping of Lophotrochozoa. The split of *R. philippinarum* was estimated at 476.9 Mya, closing to that reported by many others.

Expansion and contraction of gene families

To avoid extreme gene families, families with gene number $\geqslant$ 200 in one species and $\leqslant$ 2 in all other species were filtered at first. Cluster size of each gene family in the *R. philippinarum* genome was compared with that of C.gigas, L.gigantea, P.fucata and P.yessoensis by using Fisher exact test to identify the comparatively expansion and contraction of gene families in *R. philippinarum* to the other three species. P-value of Fisher exact test was adjusted by the false discovery rate (FDR). Judged by adjusted p-value of 0.05, 2,197 gene families significantly expanded and 3,943 gene families contracted in the *R. philippinarum* genome. (Table S18) GO enrichment and KEGG enrichment of expansion and contraction gene families in *R. philippinarum* were presented in Table S19-S22.

Positively selected genes

The protein alignments of 4,494 single-copy gene families in R.philippinarum, C.gigas, L.gigantea P.fucata and P.yessoensis were generated using MUSCLE. Gblocks (Castresana, 2000) was applied to filter poorly aligned positions and divergent regions of the protein alignments before transformed to CDS alignments. With the *R. philippinarum* as foreground branch, positive selection sites were detected based on branch-site models (Zhang et al., 2005) of PAML using the CDS alignments. P-values were computed using the $\chi 2$ statistic and adjusted by FDR method. In addition, in order to ensure the accuracy of the positive selection results, the genes with low alignment quality were filtered with the following criteria (PMID:25362486): gene length more than 300 bp, and no gap within 3 amino acids around the positive selected site in the five species. Finally, 29 positively selected genes were found in *R. philippinarum* genome. GO enrichment and KEGG enrichment of positively selected genes in *R. philippinarum* were presented in Table S23 and Table S24.

Comparative genome analysis between *R. philippinarum* and Korean Manila clam genome

The Korean Manila clam genome sequencing data (Mun et al., 2017) previously published was used to conduct the comparative analysis between the two draft Manila clam genome. Since the gene prediction of the genome of Korean clams is the genomic data (V1) without deleting heterozygosity effectively, there is a large redundancy in the resulting of 108,034 gene models. The software of HaploMerger removes the hybrid segment without interrupting the original genomic version (Huang et al., 2012). Based on which, we mapped the genome data of the last version (V2) of Korean clams to the genome of V1 version using blast. The sequences would be removed except the sequences were matched perfectly without "N". The number of genes finally obtained was 19,776 according to the gene models in the matched sequences.

Linkage map-based chromosome anchoring

A total of 20,581marker sequences with physical distance from 19 linkage group were obtained from a linkage map of *R. philippinarum* reported by Nie et al. (2017c). Only markers with a unique location were used for anchoring and orienting scaffolds to different linkage groups. Scaffolds in conflict with the genetic map (such as markers from a different linkage on the same scaffold) were checked manually with 10 kb mate-paired reads. At last, 3,888 markers were used

to construct the chromosome.

Collinearity analysis between *R. philippinarum* (Rph) and Korean clams (Hrph)

The sequences of Hrph were aligned to the genome assembly of Rph using LASTZ (version 1.02.00) with parameters "M=254 K=4500 L=3000 Y=15000 --seed=match12 --step=20 --identity=80".

RNA-seq of four color strains of *R. philippinarum*

Four selective breeding strains of *R. philippinarum* exhibiting steady and hereditary with different kinds of shell color morphs including zebra strain with brown zigzag shells (Z); white strain with white shells with a black band in the edge (W); orange strain with orange shell color (O); white zebra strain with both zigzag and white shells with a black band in the edge (WZ) (Fig.S1). The original population of different shell color including O, W, WZ, Z and partially pigmented *R. philippinarum* were selected from cultured populations in Dalian, Liaoning, China. These four selected strains were selected by 4-7 years successive generations selection and the shell color traits were steadily hereditary. One of the main functions of the mantle is to secrete biomineralization proteins to form the shell. The mantle pallial and mantle edge are the main secretory tissues. In this experiment, the mantle of four color strains was sampled for RNA extraction. Three biological replicates per each color were collected. A total amount of 3 μg RNA from mantles of each shell color strains (O, W, Z, and WZ) were used for library construction and transcriptome sequencing.

RNA-seq of different developmental stages of *R. philippinarum*

Healthy *R. philippinarum* (shell length: 3.2±0.3 cm) were collected from Zhangzidao (Dalian, Liaoning province, China) and maintained in 70 L tanks containing aerated sand-filtered seawater (salinity: 31±1 ppt, pH 8.1±0.1) at 22±1℃ for one week prior to experimentation. Artificial breeding larvae were cultivated and collected at different stages including trochophore (A11), D-shape larva (A12), umbo larva (A23) and pediveliger (Z3). The early phase of juvenile without shell color and late phase of juvenile with shell color were also sampled for RNA-seq in the orange strain and zebra strain, respectively. The collected samples were stored at -80℃ before RNA extraction.

Transcriptome response to acidification, parasite and hypoxia stress

After preliminary acclimation, one hundred clams dividing into two groups were cultured on two 70 L tank for 3 months at pH 8.0 (control) and 7.4 (treated). For water acidification, CO_2 gas was diffused directly into seawater contained in each tank to achieve testing pH conditions. Seawater pH was continuously monitored and controlled using a pH meter. Total alkalinity (TA), pH, temperature and salinity, were measured daily to determine CO_2 partial pressure (pCO_2), bicarbonate (HCO^{3-}) and carbonate (CO_3^{2-}) ions concentrations. Three biological replicates per each condition were collected.

The Manila clams were collected from the parasitic infected zone in Dalu Island. Preliminary experiments were first performed to identify the infected tissue and gonads seriously injured in the infected clams. The normal and infected gonads were selected as the samples for RNA-seq analysis. For RNA extraction, the clams were dissected in situ and the gonads were isolated from the infected and healthy individuals. Three biological replicates per each sample were collected. Then the gonads were immediately frozen in liquid nitrogen and transported in dry ice for subsequent experiments.

The experiment was performed in bottle tanks with an effective water volume of 30 L. Tanks were supplied with a continuous flow of water at 12±0.3 ℃ and 32 ppt salinity. Adult *R. philippinarum*, collected from Zhuanghe, Dalian, China, were divided into two groups of 50 animals. After a 7-day acclimatization period in tanks supplied with aerated filtered seawater, clams were exposed to hypoxia (Dissolved oxygen, DO: 2 mg/L) and normoxia (DO: 8 mg/L) as control groups. At day 0, the start of the experiment, the DO in the water was decreased to 2 mg/L using an oxygen depletion system through a fine bubble aerator where nitrogen was injected. Oxygen removal was controlled by nitrogen flow. Surface gas exchange in the rearing tank was limited by setting the water inflow under the water surface. The O2 concentration in the tank was monitored using YSI oxymeter and adjusted when necessary to keep hypoxia level constant all along the experiment. Normoxia was obtained by equilibrating seawater with air. The vitality and motility of the clams suffered no adverse affects when DO level changed and no mortality were observed either in the control or in the hypoxia-exposed clams.

Clams under hypoxia and normaxia conditions were sampled at 0, 2, 5, 8 day, respectively. Three biological replicates per each time and condition were collected. Total RNA was extracted

from the gills of 12 controls and 12 hypoxia exposed clams at 0, 2, 5, 8 days of exposure using RNAprep pure Tissue Kit (TianGene, Beijing, China), according to the manufacturer's protocol. RNA purity was determined with a NanoPhotometer® spectrophotometer (Implen, CA, USA). The RNA concentration was measured with the Qubit® RNA Assay Kit in a Qubit® 2.0 Fluorometer (Life Technologies, CA, USA). RNA integrity was assessed with the RNA Nano 6000 Assay Kit of the Agilent Bioanalyzer 2100 system (Agilent Technologies, CA, USA). Six libraries (Hypoxia and Normoxia) constructed using gills after 2 days hypoxia treatments were used for transcriptome sequencing.

Sequencing libraries and RNA-seq pipeline

In short, the extraction workflow included isolation of poly-adenylated RNA molecules using poly-T oligo-attached magnetic beads, enzymatic RNA fragmentation, cDNA synthesis, ligation of bar-coded adapters, and PCR amplification. Then, sequencing libraries were generated using NEBNext® UltraTM RNA Library Prep Kit for Illumina® (NEB, USA) following manufacturer's recommendations and index codes were added to attribute sequences to each sample. All the seven libraries were sequenced on Illumina HiSeq platform with PE150.

Sequencing reads were aligned to the *R. philippinarum* genome using hisat2 with default parameters. Gene expression levels in terms of FPKM were estimated by custom Perl scripts. Differentially expressed gene (DEG) analysis was carried out using edgeR with three biological replicates, and genes with a fold change value ≥ 2 and adjusted p-value < 0.05 were defined as significant DEGs.

Identification of the immune-related genes

The immune-related protein sets from NCBI and Uniprot (reference proteins) were searched against the five protein sets (*R.philippinarum, C. gigas, L. gigantea, P. fucata, P. yessoensis*) using BLASTP with the parameter "-e 1e-5". The genes were identified as candidates following criterion: 1) the genes have a similarity of more than 40% with the reference proteins; 2) the genes have the same domain structures with the reference proteins; 3) the annotation of the genes are same reference proteins. The motifs and domains identification of the genes were mainly performed with the Pfam and SMRT database. The genes were functionally annotated based on homologous searches against databases of NR database (NCBI).

Identification of the G protein-coupled receptor (GPCR) related genes

The protein-coding genes of *R. philippinarum*, *P. yessoensis*, *P. fucata*, *C. gigas* and *L. gigantea* were annotated based on homologous searches against the database of PFAM, NR and SwissProt. The genes with the 7 transmembrane (TM) domain were considered as the GPCR-associated family genes, that were classified into different function according the NR and SwissProt annotation. The P-values were obtained from Chi-square tests for the significant expansion gene function in the *R. philippinarum* and the total number of each function was used as background.

***R. philippinarum* and immune challenge**

Manila clams were collected from a local commercial farm and transported to the laboratory. Animals were acclimated in aerated seawater (salinity 32, temperature 20 ± 1 ℃) with 60 animals per tank (70 L, flat bottom) for 1 week prior to experimentation. After acclimation, the individuals in the experimental groups were challenged with 50 μl of immune stimulant [LPS 100 μg ml^{-1}, Poly (I:C) 100 μg ml^{-1}, and PGN 20 μg ml^{-1}, InvivoGen, USA] and the control group was injected with 50 μl PBS. Injected clams were returned to seawater tanks and four individuals from each group were randomly sampled at 0, 3, 6, 12, 24, 48, 72 and 96 h. Gill samples were collected by dissection and stored in RNAstore (Tiangen, China) until analysis by quantitative real-time RT-PCR.

Real-time RT-PCR confirmation of Illumina sequencing data

To validate our Illumina sequencing data, differentially expressed genes were selected for quantitative RT–PCR (RT–qPCR) analysis, using the same treated groups and control groups RNA samples as were used for transcriptome profiling. The primers were designed with the Primer5 software (Premier Biosoft International). The β-actin gene was used as the internal control for the qPCR analysis. RNA (500 ng) from each sample was measured and treated with RQ1 RNase-Free DNase (Promega) to remove any genomic DNA. The cDNA was synthesized from the treated RNA using a reverse transcriptase reagent kit (PrimeScript™ RT reagent Kit, Takara). The qPCR was performed with SYBR Premix Ex Taq II (Takara). The reactions were carried out in a total volume of 25 μl containing 2.5 μl of diluted cDNA, 2.5 μl of each primer, and 12.5 μl of SYBR Green PCR Master Mix, with the following cycling profile: 95 ℃ for 15 min for polymerase activation, followed by 40 cycles at 95 ℃ for 15s, at 55 ℃ for 30s, and at 70 ℃ for 30s. Each

sample was processed in triplicate in the Roche LightCycler 480 Real-Time PCR System (Roche). All data were analyzed using the $2^{-\Delta\Delta Ct}$ method.

Data availability

This genome project has been registered in NCBI under the BioProject accession PRJNA479743. The *R. philippinarum* assembly has been deposited with the accession number QUSP00000000 under PRJNA479743. All sequence data of *R. philippinarum* genome have been deposited in NCBI Sequence Read Archive under the accession numbers of SRR7716263-SRR7716297.

Supplemental References

Altschul, S.F., Madden, T.L., Schäffer, A.A., Zhang, J., Zhang, Z., Miller, W., Lipman, D.J. (1997). Gapped BLAST and PSI-BLAST: a new generation of protein database search programs. Nucleic Acids Res. 25, 3389-402

Ashburner, M., Ball, C.A., Blake, J.A., Botstein, D., Butler, H., Cherry, J.M., Davis, A.P., Dolinski, K., Dwight, S.S., Eppig, J.T., et al., (2000). Gene ontology: tool for the unification of biology. The Gene Ontology Consortium. Nat Genet. 25, 25-29

Bairoch, A., Apweiler, R. (2000). The SWISS-PROT protein sequence database and its supplement TrEMBL in 2000. Nucleic Acids Res. 28, 45-48

Benson, G. (1999). Tandem repeats finder: a program to analyze DNA sequences. Nucleic Acids Res. 27, 573-580

Birney, E., Clamp, M., and Durbin, R. (2004). Genewise and genomewise. Genome Res. 14, 988-995.

Castresana, J. (2000). Selection of conserved blocks from multiple alignments for their use in phylogenetic analysis. Mol Biol Evol 17, 540-552.

Chen, N. (2004). Using RepeatMasker to identify repetitive elements in genomic sequences. Curr Protoc Bioinformatics. Chapter 4, Unit 4

Edgar, R.C. (2004). MUSCLE: multiple sequence alignment with high accuracy and high throughput. Nucleic Acids Res. 32, 1792-1797

English, A.C., Richards, S., Han, Y., Wang, M., Vee, V., Qu, J., Qin, X., Muzny, D.M., Reid, J.G., Worley, K.C., et al., (2012). Mind the gap: upgrading genomes with Pacific Biosciences RS long-read sequencing technology. PLoS One. 7, e47748

Grabherr, M.G., Haas, B.J., Yassour, M., Levin, J.Z., Thompson, D.A., Amit, I., Adiconis, X., Fan, L., Raychowdhury R, Zeng Q, et al., (2011). Full-length transcriptome assembly from RNA-seq data without a reference genome. Nat Biotechnol. 29, 644-652

Griffiths-Jones, S., Moxon, S., Marshall, M., Khanna, A., Eddy, S. R.,, Bateman, A. (2005). Rfam: annotating non-coding RNAs in complete genomes. Nucleic Acids Res. 33, D121-124.

Haas, B.J. Salzberg, S.L., Zhu, W., Pertea, M., Allen, J.E., Orvis, J., White, O., Buell, CR., Wortman, J.R., et al., (2008). Automated eukaryotic gene structure annotation using evidence modeler and the program to assemble spliced alignments. Genome Biol. 9, R7

Haas, B.J., Delcher, A.L., Mount, S.M., Wortman, J.R., Smith Jr, R.K., Jr., Hannick, L.I., Maiti, R., Ronning, C.M., Rusch, D.B., Town, C.D. Salzberg, S.L., White, O. (2003). Improving the Arabidopsis genome annotation using maximal transcript alignment assemblies. Nucleic Acids Res, 31, 5654-5666

Hedges, S.B., Marin, J., Suleski, M., Paymer, M., Kumar, S. (2015). Tree of life reveals clock-like speciation and diversification. Mol Biol Evol. 32(4), 835-845

Huang, S., Chen, Z., Huang, G., Yu, T., Yang, P., Li, J., Fu, Y., Yuan, S., Chen, S., Xu, A. (2012). HaploMerger: Reconstructing allelic relationships for polymorphic diploid genome assemblies. Genome Res. 22, 1581-1588

Kajitani, R., Toshimoto, K., Noguchi, H., Toyoda, A., Yoshitoshi, H., Ogura, M., Okuno, M., Yabana, M., Harada, M., Nagayasu, E., Maruyama, H., et al., (2014). Efficient *de novo* assembly of highly heterozygous genomes from whole-genome shotgun short reads. Genome Res. 24, 1384-1395

Kanehisa, M., Goto, S. (2000). KEGG: kyoto encyclopedia of genes and genomes. Nucleic Acids Res. 28, 27-30

Kent, W.J. (2002). BLAT--the BLAST-like alignment tool. Genome Res. 12, 656-664

Korf, I. (2004). Gene finding in novel genomes. BMC Bioinformatics 5, 59

Li L, Stoeckert CJ Jr., Roos DS. (2003). OrthoMCL: identification of ortholog groups for eukaryotic genomes. Genome Research 13, 2178-2189.

Li, H., Durbin, R. (2009). Fast and accurate short read alignment with Burrows-Wheeler transform. Bioinformatics 25, 1754-60

Li, R., Zhu. H., Ruan, J., Qian, W., Fang, X., Shi, Z., Li, Y., Li, S., Shan, G., Kristiansen, K., Li, S., Yang, H., Wang, J., Wang, J. (2010). De novo assembly of human genomes with massively parallel short read sequencing. Genome Res. 20, 265–272.

Li, R., Fan. W., Tian, G., Zhu, H., He, L., Cai, J., Huang, Q., Cai, Q., Li, B., Bai, Y., Zhang. Z., et al., (2010). The sequence and de novo assembly of the giant panda genome. Nature. 463, 311-317.

Liu, B., Shi, Y., Yuan, J., Hu, X., Zhang, H., Li, N., Li, Z., Chen, Y., Mu, D., Fan, W. (2013). Estimation of genomic characteristics by analyzing k-mer frequency in de novo genome projects. arXiv preprint arXiv, 1308.2012,

Lowe, T.M. & Eddy, S.R. (1997). tRNAscan-SE: A Program for Improved Detection of Transfer RNA Genes in Genomic Sequence. Nucleic Acids Res. 25, 955-964

Majoros, W. H., Pertea, M., Salzberg, S. L. (2004). TigrScan and GlimmerHMM: two open-source ab initio eukaryotic gene-finders. Bioinformatics 20, 2878-2879

Mistry J., Finn R. D., Eddy S. R., Bateman A., Punta M. (2013). Challenges in Homology Search: HMMER3 and Convergent Evolution of Coiled-Coil Regions. Nucleic Acids Research, 41, e121

Mulder, N., Apweiler, R. (2007). InterPro and InterProScan: tools for protein sequence classification and comparison. Methods Mol Biol. 396, 59-70

Mun, S., Kim, Y.-J., Markkandan, K., Shin, W., Oh, S., Woo, J., et al. 2017. The whole-genome and transcriptome of the manila clam (*Ruditapes philippinarum*). Genome Biol Evol 9(6):1487-1498.

Nawrocki, E.P., Kolbe, D.L., Eddy, S.R. (2009). Infernal 1.0: inference of RNA alignments. Bioinf ormatics 25, 1335-7

Parra, G., Blanco, E., Guigo, R. (2000). GeneID in Drosophila. Genome Res. 10, 511-515

Parra, G., Bradnam, K., Korf, I. (2007). CEGMA: a pipeline to accurately annotate core genes in eukaryotic genomes. Bioinformatics. 23, 1061-7

Price, A.L., Jones, N.C., Pevzner, P.A. (2005). De novo identification of repeat families in large genomes. Bioinformatics. 21 Suppl 1, 351-358

Salamov, A.A., Solovyev, V.V. (2000). Ab initio gene finding in Drosophila genomic DNA. Genome Res. 10, 516–522.

Simakov, O., Kawashima, T., Marlétaz, F., Jenkins, J., Koyanagi, R., Mitros, T., Hisata, K., Bredeson, J., Shoguchi, E., Gyoja, F., Yue, J.X., Chen, Y.C., Freeman, R.M. Jr, Sasaki A. (2015). Hemichordate genomes and deuterostome origins. Nature. 527(7579), 459-465.

Simao, F.A., Waterhouse, R.M., Ioannidis, P., Kriventseva, E.V., Zdobnov, E.M. (2015). BUSCO: assessing genome assembly and annotation completeness with single-copy orthologs. Bioinformatics. 31, 3210–3212.

Smit, A. F. A., Hubley, R., Green, P. RepeatMasker at < http://www.repeatmasker.org/RepeatModeler.html >.

Stamatakis, A. (2006). RAxML-VI-HPC: maximum likelihood-based phylogenetic analyses with thousands of taxa and mixed models. Bioinformatics 22, 2688–2690

Stamatakis, A., Hoover, P., Rougemont, J. (2008). A rapid bootstrap algorithm for the RAxML web servers. Syst. Biol. 57, 758–771

Stanke, M., Waack, S. (2003). Gene prediction with a hidden Markov model and a new intron submodel. Bioinformatics 19, ii215–225

Stanke, M., Schoffmann, O., Morgenstern, B., Waack, S. (2006). Gene prediction in eukaryotes with a generalized hidden Markov model that uses hints from external sources. BMC Bioinformatics 7, 62

Trapnell, C., Williams, B.A., Pertea, G., Mortazavi, A., Kwan, G., van Baren, M.J., Salzberg, S.L., Wold, B.J., Pachter, L. (2010). Transcript assembly and quantification by RNA-Seq reveals unannotated transcripts and isoform switching during cell differentiation. Nat. Biotechnol. 28, 511

Trapnell, C., Pachter, L., Salzberg, S. L. (2009). TopHat: Discovering splice junctions with RNA-Seq. Bioinformatics 25, 1105-1111

Xu, Z., Wang, H. (2007). Ltr_finder: an efficient tool for the prediction of full-length ltr retrotransposons. Nucl. Acids Res. 35, W265-268

Yang, Z. (2007). PAML 4: phylogenetic analysis by maximum likelihood. Mol Biol Evol. 24, 1586–1591

Yu, X.J., Zheng, H.K., Wang, J., Wang, W., Su, B. (2006). Detecting lineage-specific adaptive evolution of brain-expressed genes in human using rhesus macaque as outgroup. Genomics 88, 745-751

Zhang, J., Nielsen, R., Yang, Z. (2005). Evaluation of an Improved Branch-Site Likelihood Method for Detecting Positive Selection at the Molecular Level. Mol Biol Evol. 22, 2472-2479

Table S1 Statistics for K-mer analysis of *R. philippinarum* genome. Related to Figure 1.

K-mer	K-mer Number	K-mer Depth	Genome Size (Mb)	Heterozygous Ratio (%)
17	50,054,797,752	38	1,317.23	2.00

Table S2 Genome sequencing of *R. philippinarum*. Related to Figure 1.

Platform	Insert size	Read length (bp)	Raw data (G)	Sequence coverage
Illumina	230 bp	125	91.5	69.48
	300 bp	125	95.7	72.67
	500 bp	125	98.9	75.90
	2 Kbp	125	57.9	43.96
	5 Kbp	125	39.6	30.07
	10 Kbp	125	13.1	9.95
	20 Kbp	125	24.5	18.60
	Total		421.2	320.63

Note: The estimated genome size is ~1.32G, and sequence coverage = Total clean bases/1.32G.

Table S3 Statistics of the assembly of the *R. philippinarum* genome. Related to Figure 1.

Sample ID	Length		Number	
	Contig (bp)	Scaffold (>100 bp)	Contig	Scaffold (>100 bp)
Total	1,062,832,364	1,122,973,377	88,274	30,811
Max	249,659	2,001,120	-	-

Number>=100	-	-	88,188	30,811
Number>=2000	-	-	61,395	12,134
N50	28,111	345,005	10,827	954
N60	21,924	273,959	15,106	1,317
N70	16,368	193,236	20,718	1,804
N80	11,299	122,382	28,507	2,532
N90	6,270	51,774	40,880	3,897

Note: Only the length of scaffold greater than 100 bp was counted. N50 refers to the length of sequence equal to or greater than the half of total sequences length.

Table S4 The number of SNPs and genome annotation characterization of wild and inbred *R. philippinarum*. Related to Figure 1.

Sample	Upstream	Exonic				Intronic	Splicing	Downstream	Upstream/Downstream	Intergenic	Het rate(%)	Total
		Stop gain	Stop loss	Synonymous	Non-synonymous							
Wild	737,992	6,915	1,070	752,893	483,383	9,463,918	2,290	882,366	23,143	21,459,387	1.690	33,830,021
Inbred	266,777	1,268	444	365,185	175,823	3,488,425	870	303,942	9,028	7,061,957	1.038	11,758,346

Table S5 Statistics of genome content. The table shows GC content of *R. philippinarum* genome. Related to Figure 1.

	Number (bp)	% of genome
A	361,902,804	32.23
T	361,997,214	32.24

C	169,455,540	15.09
G	169,476,806	15.09
N	60,141,013	5.36
GC	367,211,996	31.89
Total (bp)	1,122,973,377	100

Note: GC content of the genome without N.

Table S6 Assessment the genome coverage rate using raw data. Related to Figure 1.

	Sample ID	Percentage
Reads	Mapping rate (%)	93.32
	Average sequencing depth	137.3
	Coverage (%)	99.83
Genome	Coverage at least 4X (%)	99.55
	Coverage at least 10X (%)	99.08
	Coverage at least 20X (%)	98.27

Table S7 Assessment the gene coverage rate using EST data. Related to Figure 1.

Dataset	Number	Total length (bp)	Sequences covered by assembly	with >90% sequence in one scaffold		with >50% sequence in one scaffold	
				Number	Percent (%)	Number	Percent (%)
>200 bp	44,321	34,136,266	99.75	36,129	81.52	43,706	98.61
>500 bp	18,197	26,149,430	99.89	14,560	80.01	17,977	98.79
>1 Kbp	9,056	19,790,574	99.98	7,066	78.03	8,930	98.61
>2 Kbp	3,626	12,154,398	99.97	2,807	77.41	3,558	98.12

Table S8 CEGMA results of *R. philippinarum* genome. Related to Figure 1.

Species	Complete		Complete + partial	
	Prots	% completeness	Prots	% completeness
R. philippinarum	214	86.29%	233	93.95%

Note: CEGMA (Core Eukaryotic Genes Mapping Approach) defined the number of 248 ultra-conserved CEGs that occur in a wide range of eukaryotes. A protein is classified as complete if the alignment of the predicted protein to the HMM profile represents at least 70% of the original KOG domain, otherwise is classified as partial.

Table S9 BUSCO (Benchmarking Universal Single-Copy Orthologs) results of *R. philippinarum* genome. Related to Figure 1.

Species	Size	BUSCO notation assessment results
R. philippinarum	1123Mbp	C:92.2%[S:90.3%,D:1.9%],F:1.6%,M:6.2%,n:978

Note: The recovered matches were classified as 'complete' (C) if their lengths were within the expectation of the BUSCO profile match lengths. If these were found more than once they were classified as 'duplicated'(D). The matches that were only partially recovered were classified as 'fragmented'(F), and BUSCO groups for which there were no matches that pass the tests of orthology were classified as 'missing'(M).The number of total BUSCO groups (n) was 843.

Table S10 The prediction of repeats elements in *R. philippinarum* genome. Related to Figure 1.

Type	Repeat Size (bp)	Percent (%)
TRF	69,164,254	6.16
RepeatMasker	389,644,949	34.70
RepeatProteinMask	26,094,608	2.32
Total	430,065,124	38.30

Note: Repeats in *R. philippinarum* genome were consisted with tendam repeats and interpersed repeats. The TRF (Tandem repeats finder) was used to predict tandem repeats, RepeatMasker and RepeatProteinMask were used to predict interpersed repeats.

Table S11 Categories of TEs predicted in *R. philippinarum* genome. Related to Figure 1.

		Repeatmasker		TE Proteins		Combined TEs	
		Length (bp)	% in Genome	Length (bp)	% in Genome	Length (bp)	% in Genome
DNA transposon	DNA	212,422,142	18.916	6,059,255	0.54	216,075,767	19.241
Retrotransposon	LINE	53,578,378	4.771	15,019,016	1.337	61,586,774	5.484
	LTR	104,648,756	9.319	5,050,079	0.45	107,571,925	9.579
	SINE	3,507,191	0.312	0	0	3,507,191	0.312
Other	Other*	268	0.000024	0	0	268	0.000024
	Unknown*	60,134,172	5.355	0	0	60,134,172	5.355
	Total	389,644,949	34.698	26,094,608	2.324	402,086,301	35.806

Note: The genomic abundance of TEs were predicted by Repeatmasker through ab-initio method and homology based method. The TE proteins were predicted based on TE protein database by RepeatProteinMask. The final results of TEs in *R. philippinarum* genome were integrated of both methods without redundancy. "Other" refer to the repeats that can be classified by RepeatMasker, but not included by the classes above; "Unknown" refer to the repeats that can't be classified by RepeatMasker.

Table S12 General statistics of predicted protein-coding genes. Related to Figure 1.

Gene set		Number	Average transcript length (bp)	Average CDS length (bp)	Average exons per gene	Average exon length (bp)	Average intron length (bp)
De novo[#]	Augustus	37,212	8970.26	1318.06	6.09	216.40	1503.11
	Genscan	33,272	17857.67	1311.80	5.45	240.77	3719.46
	GlimmerHMM	101,946	9113.13	590.15	3.68	160.29	3178.12
	SNAP	93,644	10462.10	760.63	5.74	132.41	2044.87
	Geneid	51,889	9438.01	791.52	3.19	248.49	3956.73

Homolog[$]	*Anopheles gambiae*	7,026	5620.28	910.20	4.13	220.15	1502.66
	Caenorhabditis elegans	5,354	4708.19	850.06	3.46	245.65	1568.09
	Crassostrea gigas	22,191	5354.00	947.14	4.03	235.31	1456.81
	Capitella teleta	25,597	3394.37	683.32	2.91	234.60	1417.38
	Drosophila melanogaster	6,136	6097.26	960.26	4.44	216.50	1495.29
	Helobdella robusta	16,268	3246.21	654.20	2.75	237.65	1478.81
	Lingula anatina	20,212	4490.71	894.63	3.60	248.76	1385.09
	Lottia gigantea	29,596	3678.82	744.03	3.14	236.65	1368.86
	Octopus bimaculoides	19,075	3190.45	703.71	2.85	247.09	1345.62
	Strongylocentrotus purpuratus	17,087	3085.22	784.98	2.77	283.62	1301.29
RNA_Seq	Cufflinks	68,334	13341.41	2150.26	6.00	358.12	2236.31
	PASA	16,620	16879.93	1361.17	6.41	212.19	2163.52
	EVM	39,527	9980.28	1274.46	6.12	208.18	1699.73
	PASA update	39,348	10520.53	1283.68	6.15	208.74	1690.74
	Final set *	27,652	12875.81	1462.72	7.30	200.30	1697.30

Note: # Statistics calculated from the gene set predicted form each method. $ Statistics calculated from the gene set predicted by homolog proteins from each species.
* Statistics calculated from the *R.philippinarum* genome.

Table S13 General statistics of protein-coding genes of homolog species. Related to Figure 1.

Species	Number	Average transcript length (bp)	Average CDS length (bp)	Average exons per gene	Average exon length (bp)	Average intron length (bp)
Ruditapes philippinarum	27,652	12875.81	1462.72	7.30	200.30	1697.30
Crassostrea gigas	26,089	8072.40	1344.93	7.16	187.75	1091.49
Capitella teleta	31,440	2652.33	1074.05	5.37	200.03	361.20

Helobdella robusta	23,350	3762.63	1127.79	5.99	188.43	528.50
Lingula anatina	32,828	6526.03	1414.25	7.51	188.26	784.94
Lottia gigantea	23,205	5045.43	1150.31	6.01	191.37	777.29
Octopus bimaculoides	30,845	8553.10	779.28	3.59	217.04	3000.89

Table S14 General statistics of mapping rate to functional database of protein-coding genes. Related to Figure 1.

	Number	Percent (%)
Total	27,652	-
Swissprot	19,774	71.51
TrEMBL	23,875	86.34
NR	24,124	87.24
KEGG	18,626	67.36
InterPro	19,625	70.97
GO	15,084	54.55
Pfam	18,952	68.54
Annotated	24,570	88.85
Unannotated	3,082	11.15

Table S15 General statistics of non-coding RNA of the genome. Related to Figure 1.

Type	Number	Average length (bp)	Total length (bp)	% of genome
miRNA	600	109.16	65,497	0.0058
tRNA	3,788	78.15	296,030	0.0264

rRNA	rRNA	24	161.96	3,887	0.0003
	18S	17	184.29	3,133	0.0003
	28S	3	130.67	392	0.00004
	5.8S	4	87.75	351	0.000031
	5S	4	90.5	362	0.00003
snRNA	snRNA	158	136.67	21,594	0.0019
	CD-box	42	101.36	4,257	0.0004
	HACA-box	21	191.9	4,030	0.0004
	splicing	90	137.38	12,364	0.0011

Table S16 GO enrichment of expanded gene families in Rph compared with Hrph. Related to Table 1.

GO ID	GO Term	GO Class	P-value	Adjusted P-value	Gene Number
GO:0005215	transporter activity	MF	1.53E-67	3.45E-65	58
GO:0051179	localization	BP	8.56E-57	6.45E-55	69
GO:0044765	single-organism transport	BP	3.75E-54	2.12E-52	58
GO:0022804	active transmembrane transporter activity	MF	1.08E-48	4.90E-47	41
GO:0016887	ATPase activity	MF	1.99E-38	6.43E-37	36
GO:0030286	dynein complex	CC	2.40E-37	5.43E-36	19
GO:0005524	ATP binding	MF	1.09E-32	2.24E-31	39
GO:0055085	transmembrane transport	BP	6.12E-31	9.88E-30	32
GO:0003777	microtubule motor activity	MF	4.91E-30	7.39E-29	22
GO:0007018	microtubule-based movement	BP	4.64E-29	6.27E-28	22
GO:0042626	ATPase activity, coupled to transmembrane movement of substances	MF	5.27E-29	6.27E-28	20
GO:0017111	nucleoside-triphosphatase activity	MF	1.55E-28	1.67E-27	42
GO:0005328	neurotransmitter:sodium symporter activity	MF	8.48E-28	7.10E-27	21

GO:0006836	neurotransmitter transport	BP	1.55E-27	1.25E-26	21
GO:0000166	nucleotide binding	MF	9.87E-25	7.19E-24	45
GO:0044699	single-organism process	BP	8.68E-24	5.45E-23	90
GO:0001539	cilium or flagellum-dependent cell motility	BP	2.46E-23	1.46E-22	11
GO:0005858	axonemal dynein complex	CC	3.37E-21	1.65E-20	10
GO:0016020	membrane	CC	4.96E-18	1.65E-17	68
GO:0007160	cell-matrix adhesion	BP	1.55E-16	4.92E-16	11
GO:0022892	substrate-specific transporter activity	MF	8.96E-16	2.81E-15	26
GO:0016787	hydrolase activity	MF	8.53E-15	2.54E-14	43
GO:0044763	single-organism cellular process	BP	1.49E-14	4.31E-14	64
GO:0016021	integral component of membrane	CC	2.01E-13	5.67E-13	46
GO:0005509	calcium ion binding	MF	5.73E-11	1.52E-10	21
GO:0009190	cyclic nucleotide biosynthetic process	BP	4.21E-10	1.06E-09	9
GO:0016849	phosphorus-oxygen lyase activity	MF	4.21E-10	1.06E-09	9
GO:0043167	ion binding	MF	2.36E-09	5.62E-09	60
GO:0005044	scavenger receptor activity	MF	2.38E-08	5.43E-08	9
GO:0009987	cellular process	BP	4.78E-06	1.01E-05	65
GO:0005319	lipid transporter activity	MF	6.20E-06	1.30E-05	5
GO:0006869	lipid transport	BP	7.12E-06	1.46E-05	5
GO:0004713	protein tyrosine kinase activity	MF	8.90E-04	1.69E-03	9
GO:0003824	catalytic activity	MF	2.54E-03	4.62E-03	53
GO:0035556	intracellular signal transduction	BP	5.24E-03	9.33E-03	9
GO:0006468	protein phosphorylation	BP	5.88E-03	1.04E-02	9
GO:0008281	sulfonylurea receptor activity	MF	7.36E-03	1.29E-02	1

Table S17 GO enrichment of unique gene families in *R. philippinarum* compared with four other Mollusca species (*C. gigas, L. gigantea, P. fucata* and *P. yessoensis*). Related to Figure 1.

Table S18 KEGG enrichment of unique gene families in *R. philippinarum* compared with four other Mollusca species (*C. gigas, L. gigantea, P. fucata* and *P. yessoensis*). Related to Figure 1.

Map ID	MapTitle	P-value	Adjusted P-value	Gene Number
map04080	Neuroactive ligand-receptor interaction	3.21E-55	8.98E-53	321
map04512	ECM-receptor interaction	2.24E-16	3.14E-14	144
map00513	Various types of N-glycan biosynthesis	6.84E-12	6.39E-10	74
map05206	MicroRNAs in cancer	1.11E-11	7.54E-10	115
map04510	Focal adhesion	1.35E-11	7.54E-10	191
map04151	PI3K-Akt signaling pathway	6.12E-09	2.63E-07	170
map04540	Gap junction	6.57E-09	2.63E-07	64
map05033	Nicotine addiction	1.01E-08	3.54E-07	41
map00601	Glycosphingolipid biosynthesis - lacto and neolacto series	1.68E-08	5.24E-07	35
map04725	Cholinergic synapse	5.62E-08	1.57E-06	66
map04514	Cell adhesion molecules (CAMs)	7.89E-08	2.01E-06	53
map05130	Pathogenic	1.42E-07	3.32E-06	53

	Escherichia coli infection			
map05204	Chemical carcinogenesis	1.77E-06	3.31E-05	45
map00906	Carotenoid biosynthesis	3.05E-06	5.03E-05	11
map04672	Intestinal immune network for IgA production	2.74E-05	3.48E-04	8
map04145	Phagosome	6.36E-05	6.59E-04	102
map04974	Protein digestion and absorption	3.69E-04	2.92E-03	85
map05145	Toxoplasmosis	1.19E-03	7.89E-03	72
map05020	Prion diseases	1.21E-03	7.89E-03	29
map04913	Ovarian steroidogenesis	1.27E-03	7.92E-03	28
map00100	Steroid biosynthesis	1.47E-03	8.78E-03	18
map04726	Serotonergic synapse	1.72E-03	9.83E-03	46
map04610	Complement and coagulation cascades	2.07E-03	1.09E-02	52
map04020	Calcium signaling pathway	3.29E-03	1.56E-02	104
map04115	p53 signaling pathway	5.73E-03	2.40E-02	39
map00533	Glycosaminoglycan biosynthesis - keratan	5.93E-03	2.44E-02	20

	sulfate			
map00534	Glycosaminoglycan biosynthesis - heparan sulfate / heparin	8.90E-03	3.32E-02	15
map00140	Steroid hormone biosynthesis	9.19E-03	3.37E-02	26
map05222	Small cell lung cancer	9.90E-03	3.51E-02	58
map04210	Apoptosis	1.18E-02	4.04E-02	49

Table S19 GO enrichment of expanded gene families in *R. philippinarum* compared with four other Mollusca species (*C. gigas, L. gigantea, P. fucata* and *P. yessoensis*). Related to Figure 1.

Table S20 KEGG enrichment of expanded gene families in *R. philippinarum* compared with four other Mollusca species (*C. gigas, L. gigantea, P. fucata* and *P. yessoensis*). Related to Figure 1.

Map ID	MapTitle	P-value	Adjusted P-value	Gene Number
map04080	Neuroactive ligand-receptor interaction	2.38E-67	7.09E-65	420
map04512	ECM-receptor interaction	4.11E-47	6.12E-45	237
map04151	PI3K-Akt signaling pathway	6.99E-30	6.95E-28	279
map04510	Focal adhesion	2.58E-27	1.92E-25	291
map04974	Protein digestion and absorption	4.46E-23	2.66E-21	160

map05146	Amoebiasis	7.03E-19	3.49E-17	136
map04610	Complement and coagulation cascades	1.41E-14	6.02E-13	95
map05322	Systemic lupus erythematosus	4.23E-12	1.58E-10	74
map05150	Staphylococcus aureus infection	6.21E-12	2.05E-10	73
map04514	Cell adhesion molecules (CAMs)	4.71E-10	1.40E-08	71
map04725	Cholinergic synapse	5.70E-10	1.50E-08	88
map05020	Prion diseases	6.04E-10	1.50E-08	49
map05204	Chemical carcinogenesis	1.31E-08	2.68E-07	61
map04611	Platelet activation	2.44E-08	4.27E-07	130
map04145	Phagosome	9.81E-08	1.33E-06	144
map00513	Various types of N-glycan biosynthesis	2.45E-07	2.92E-06	82
map04640	Hematopoietic cell lineage	9.99E-07	1.03E-05	38
map03450	Non-homologous end-joining	1.64E-06	1.57E-05	30
map05206	MicroRNAs in cancer	2.38E-06	2.22E-05	129

map05033	Nicotine addiction	3.32E-06	3.00E-05	46
map00906	Carotenoid biosynthesis	7.85E-06	6.16E-05	12
map05222	Small cell lung cancer	1.00E-05	7.65E-05	88
map04020	Calcium signaling pathway	3.34E-05	2.17E-04	148
map00532	Glycosaminoglycan biosynthesis - chondroitin sulfate / dermatan sulfate	6.93E-05	4.17E-04	45
map05144	Malaria	1.18E-04	6.77E-04	38
map05130	Pathogenic Escherichia coli infection	5.13E-04	2.22E-03	57
map00140	Steroid hormone biosynthesis	1.04E-03	3.73E-03	36
map04623	Cytosolic DNA-sensing pathway	2.51E-03	8.39E-03	38
map05145	Toxoplasmosis	2.72E-03	8.77E-03	92
map04672	Intestinal immune network for IgA production	2.74E-03	8.77E-03	7
map04110	Cell cycle	2.95E-03	9.26E-03	74
map05142	Chagas disease	3.60E-03	1.12E-02	54

	(American trypanosomiasis)			
map05161	Hepatitis B	5.39E-03	1.59E-02	70
map05133	Pertussis	7.62E-03	2.10E-02	88
map04540	Gap junction	7.73E-03	2.11E-02	62
map05310	Asthma	8.12E-03	2.14E-02	6
map00980	Metabolism of xenobiotics by cytochrome P450	8.19E-03	2.14E-02	34
map05164	Influenza A	1.25E-02	2.98E-02	93
map04668	TNF signaling pathway	1.43E-02	3.33E-02	49
map05323	Rheumatoid arthritis	1.70E-02	3.84E-02	30
map04977	Vitamin digestion and absorption	2.08E-02	4.50E-02	30

Table S21 GO enrichment of contracted gene families in *R. philippinarum* compared with four other Mollusca species (*C. gigas, L. gigantea, P. fucata* and *P. yessoensis*). Related to Figure 1.

GO ID	GO Term	GO Class	P-value	Adjusted P-value	Gene Number
GO:0007155	cell adhesion	BP	1.71E-06	1.89E-04	7
GO:0000786	nucleosome	CC	1.30E-05	4.66E-04	3
GO:0006334	nucleosome assembly	BP	2.18E-05	4.66E-04	3
GO:0004527	exonuclease activity	MF	4.96E-05	6.86E-04	3

GO:0004867	serine-type endopeptidase inhibitor activity	MF	8.13E-05	1.06E-03	3
GO:0006352	DNA-templated transcription, initiation	BP	1.95E-03	1.49E-02	2

Table S22 KEGG enrichment of contracted gene families in *R. philippinarum* compared with four other Mollusca species (*C. gigas, L. gigantea, P. fucata* and *P. yessoensis*). Related to Figure 1.

Map ID	MapTitle	P-value	Adjusted P-value	Gene Number
map04512	ECM-receptor interaction	4.29E-08	2.56E-06	11
map04510	Focal adhesion	5.56E-08	2.56E-06	13
map04151	PI3K-Akt signaling pathway	1.89E-06	5.79E-05	11
map05146	Amoebiasis	2.27E-05	5.22E-04	7
map04974	Protein digestion and absorption	4.85E-04	6.70E-03	6
map05200	Pathways in cancer	5.22E-04	6.70E-03	7
map00860	Porphyrin and chlorophyll metabolism	5.55E-04	6.70E-03	3
map04611	Platelet activation	5.82E-04	6.70E-03	6
map00053	Ascorbate and aldarate metabolism	7.93E-04	8.02E-03	3

map05221	Acute myeloid leukemia	8.72E-04	8.02E-03	3
map05322	Systemic lupus erythematosus	1.11E-03	9.32E-03	4
map04120	Ubiquitin mediated proteolysis	1.54E-03	1.10E-02	5
map00983	Drug metabolism - other enzymes	1.62E-03	1.10E-02	3
map00040	Pentose and glucuronate interconversions	1.68E-03	1.10E-02	3
map05202	Transcriptional misregulation in cancer	1.79E-03	1.10E-02	4
map05164	Influenza A	2.10E-03	1.21E-02	5
map00140	Steroid hormone biosynthesis	2.60E-03	1.41E-02	3
map00980	Metabolism of xenobiotics by cytochrome P450	2.76E-03	1.41E-02	3
map04610	Complement and coagulation cascades	2.96E-03	1.43E-02	4
map05034	Alcoholism	3.12E-03	1.43E-02	4
map00830	Retinol metabolism	3.58E-03	1.57E-02	3
map05168	Herpes simplex	4.02E-03	1.68E-02	4

	infection			
map00500	Starch and sucrose metabolism	4.87E-03	1.88E-02	3
map05206	MicroRNAs in cancer	4.91E-03	1.88E-02	5
map00982	Drug metabolism - cytochrome P450	5.11E-03	1.88E-02	3
map05204	Chemical carcinogenesis	7.60E-03	2.69E-02	3
map05150	Staphylococcus aureus infection	1.05E-02	3.58E-02	3
map04064	NF-kappa B signaling pathway	1.27E-02	4.17E-02	3
map04726	Serotonergic synapse	1.46E-02	4.65E-02	3

Table S23 GO enrichment of positively selected genes in *R. philippinarum* compared with four other Mollusca species (*C. gigas, L. gigantea, P. fucata* and *P. yessoensis*). Related to Figure 1.

GO ID	GO Term	GO Class	P-value	Adjusted P-value	Gene Number
GO:0046034	ATP metabolic process	BP	7.98E-09	2.43E-06	4
GO:0016820	hydrolase activity, acting on acid anhydrides, catalyzing transmembrane movement of substances	MF	2.48E-08	2.43E-06	5
GO:1902600	hydrogen ion transmembrane transport	BP	2.95E-08	2.43E-06	4
GO:0033178	proton-transporting two-sector ATPase complex, catalytic domain	CC	2.25E-07	7.72E-06	3

GO:0009205	purine ribonucleoside triphosphate metabolic process	BP	4.57E-07	1.15E-05	6
GO:0046128	purine ribonucleoside metabolic process	BP	5.82E-07	1.25E-05	6
GO:0009150	purine ribonucleotide metabolic process	BP	1.14E-06	1.68E-05	6
GO:0015991	ATP hydrolysis coupled proton transport	BP	1.21E-06	1.68E-05	3
GO:0016817	hydrolase activity, acting on acid anhydrides	MF	4.12E-06	4.55E-05	8
GO:0006812	cation transport	BP	4.70E-05	4.36E-04	5
GO:0006810	transport	BP	1.10E-04	9.84E-04	10
GO:0008060	ARF GTPase activator activity	MF	1.33E-04	1.04E-03	2
GO:0032312	regulation of ARF GTPase activity	BP	1.33E-04	1.04E-03	2
GO:1901363	heterocyclic compound binding	MF	1.48E-04	1.10E-03	12
GO:0050790	regulation of catalytic activity	BP	1.50E-04	1.10E-03	3
GO:0097159	organic cyclic compound binding	MF	1.51E-04	1.10E-03	12
GO:0019220	regulation of phosphate metabolic process	BP	1.98E-04	1.32E-03	3
GO:0000166	nucleotide binding	MF	2.00E-04	1.32E-03	9
GO:0006139	nucleobase-containing compound metabolic process	BP	3.16E-04	1.93E-03	8
GO:0006796	phosphate-containing compound metabolic process	BP	3.80E-04	2.24E-03	7
GO:0005524	ATP binding	MF	3.94E-04	2.26E-03	7
GO:0019829	cation-transporting ATPase activity	MF	4.61E-04	2.31E-03	2

GO:0035639	purine ribonucleoside triphosphate binding	MF	4.66E-04	2.31E-03	8
GO:0032550	purine ribonucleoside binding	MF	4.77E-04	2.31E-03	8
GO:0032555	purine ribonucleotide binding	MF	4.77E-04	2.31E-03	8
GO:0030117	membrane coat	CC	7.50E-04	3.26E-03	2
GO:0015031	protein transport	BP	7.64E-04	3.28E-03	4
GO:0016787	hydrolase activity	MF	1.27E-03	5.25E-03	9
GO:0051017	actin filament bundle assembly	BP	1.46E-03	5.69E-03	1
GO:0051764	actin crosslink formation	BP	1.46E-03	5.69E-03	1
GO:0043234	protein complex	CC	1.51E-03	5.83E-03	5
GO:0006886	intracellular protein transport	BP	2.04E-03	7.63E-03	3
GO:0017111	nucleoside-triphosphatase activity	MF	2.34E-03	7.86E-03	5
GO:0004127	cytidylate kinase activity	MF	2.92E-03	9.17E-03	1
GO:0010389	regulation of G2/M transition of mitotic cell cycle	BP	4.37E-03	1.22E-02	1
GO:0044237	cellular metabolic process	BP	4.46E-03	1.22E-02	10
GO:0004017	adenylate kinase activity	MF	5.82E-03	1.55E-02	1
GO:0016192	vesicle-mediated transport	BP	5.99E-03	1.58E-02	2
GO:0046933	proton-transporting ATP synthase activity, rotational mechanism	MF	7.27E-03	1.88E-02	1
GO:0005488	binding	MF	1.05E-02	2.60E-02	19
GO:0015986	ATP synthesis coupled proton transport	BP	1.31E-02	3.11E-02	1
GO:0000079	regulation of cyclin-dependent protein serine/threonine kinase activity	BP	1.31E-02	3.11E-02	1
GO:0019901	protein kinase binding	MF	1.31E-02	3.11E-02	1
GO:0030131	clathrin adaptor complex	CC	1.74E-02	3.87E-02	1

Table S24 KEGG enrichment of positively selected genes in *R. philippinarum* compared with four other Mollusca species (*C. gigas, L. gigantea, P. fucata* and *P. yessoensis*). Related to Figure 1.

Map ID	MapTitle	P-value	Adjusted P-value	Gene Number
map00190	Oxidative phosphorylation	9.72E-06	3.60E-04	4
map04966	Collecting duct acid secretion	2.68E-04	4.96E-03	2
map04144	Endocytosis	1.37E-03	1.69E-02	4
map04721	Synaptic vesicle cycle	5.42E-03	3.98E-02	2
map05110	Vibrio cholerae infection	6.03E-03	3.98E-02	2
map05323	Rheumatoid arthritis	7.32E-03	3.98E-02	2
map05010	Alzheimer's disease	7.53E-03	3.98E-02	3
map05120	Epithelial cell signaling in Helicobacter pylori infection	1.06E-02	4.92E-02	2

Table S25 Immune related GO enrichment in *R. philippinarum*. Related to Figure 3.

Table S26 Immune related KEGG enrichment in *R. philippinarum*. Related to Figure 3.

Map ID	MapTitle	P-value	Adjusted P-value	Gene Number
map04512	ECM-receptor interaction	5.40E-58	1.25E-55	210
map04151	PI3K-Akt signaling pathway	6.11E-43	7.08E-41	250
map04974	Protein digestion and absorption	7.74E-41	5.98E-39	156
map04080	Neuroactive ligand-receptor interaction	4.35E-38	2.52E-36	298

map05146	Amoebiasis	6.16E-34	2.86E-32	133
map04510	Focal adhesion	8.31E-33	3.21E-31	247
map05150	Staphylococcus aureus infection	6.62E-21	2.19E-19	72
map05020	Prion diseases	3.74E-18	1.08E-16	50
map05142	Chagas disease (American trypanosomiasis)	6.74E-17	1.74E-15	69
map04610	Complement and coagulation cascades	4.61E-15	1.07E-13	79
map04145	Phagosome	1.19E-14	2.50E-13	133
map04611	Platelet activation	1.83E-14	3.53E-13	119
map00513	Various types of N-glycan biosynthesis	2.99E-13	5.33E-12	78
map04514	Cell adhesion molecules (CAMs)	5.18E-13	8.58E-12	63
map00601	Glycosphingolipid biosynthesis - lacto and neolacto series	9.41E-13	1.43E-11	41
map04640	Hematopoietic cell lineage	9.83E-13	1.43E-11	39
map00532	Glycosaminoglycan biosynthesis - chondroitin sulfate / dermatan sulfate	1.46E-12	1.99E-11	49
map05322	Systemic lupus erythematosus	4.51E-12	5.51E-11	61
map00603	Glycosphingolipid biosynthesis - globo series	1.46E-11	1.69E-10	31

map05140	Leishmaniasis	2.24E-10	1.92E-09	36
map05145	Toxoplasmosis	3.85E-09	3.08E-08	91
map05222	Small cell lung cancer	4.49E-09	3.36E-08	79
map05133	Pertussis	9.39E-08	5.89E-07	86
map04725	Cholinergic synapse	6.66E-07	3.51E-06	65
map05144	Malaria	6.99E-07	3.60E-06	35
map05152	Tuberculosis	3.40E-06	1.61E-05	102
map00533	Glycosaminoglycan biosynthesis - keratan sulfate	5.13E-06	2.34E-05	26
map05162	Measles	1.29E-05	5.46E-05	60
map04210	Apoptosis	1.58E-05	6.45E-05	60
map05321	Inflammatory bowel disease (IBD)	1.89E-05	7.32E-05	19
map00960	Tropane, piperidine and pyridine alkaloid biosynthesis	3.38E-05	0.000124404	12
map03450	Non-homologous end-joining	3.62E-05	0.000131329	23
map04620	Toll-like receptor signaling pathway	4.50E-05	0.000160671	49
map04064	NF-kappa B signaling pathway	8.42E-05	0.000279211	49
map00906	Carotenoid biosynthesis	0.000343364	0.000995755	9
map00950	Isoquinoline alkaloid biosynthesis	0.000587249	0.001621925	18

map00600	Sphingolipid metabolism	0.00082273	0.002169015	33
map00965	Betalain biosynthesis	0.000889029	0.002291719	12
map05033	Nicotine addiction	0.001312885	0.003206205	32
map05206	MicroRNAs in cancer	0.001685051	0.0039891	91
map05310	Asthma	0.001727778	0.004048933	6
map00061	Fatty acid biosynthesis	0.004821937	0.010553674	11
map04668	TNF signaling pathway	0.006544757	0.013803487	40
map05012	Parkinson's disease	0.00867672	0.017657886	40
map05323	Rheumatoid arthritis	0.017005693	0.032877674	24

Table S27 The gene number of TEP superfamily in different species. Related to Figure 3.

Gene	*R. philippinarum*	*C. gigas*	*P. fucata*	*L. gigantea*	*P. yesoensis*
C3	7	1	1	1	1
CD109	17	4	9	6	5
A2M	2	2	1	2	1

Table S28 RNA-seq differentially expressed genes (DEGs) under hypoxia exposure. Related to Figure 2.

Table S29 RNA-seq differentially expressed genes (DEGs) of *R. philippinarum* gonads exposed to digenetic trematode in nature. Related to Figure 2.

Table S30 The classified statistics of the GPCR-associated genes in the *R. philippinarum*, *P. yessoensis*, *C. gigas*, *P. fucata* and *L. gigantea*. Related to Figure 4.

Note: red indicates the expansion of the GPCR genes in Manila clam, and blue indicates genes uniquely observed in Manila clam.

Table S31 GO enrichment of expanded gene families in Rph compared with Hrph. Related to Table 1.

species	length	contig N50	scaffold N50	BUSCO（genome）
R. philippinarum	1.12 Gb	28.1 Kb	345.0 Kb	C:92.2% [S:90.3%, D:1.9%], F:1.6%, M:6.2%, n:978
B. platifrons	1.66 Gb	13.2 Kb	343.4 Kb	C:93.2% [S:91.9%, D:1.3%], F:2.6%, M:4.2%, n:978
M. philippinarum	2.63 Gb	19.7 Kb	100.2 Kb	C:88.9% [S:86.0%, D:2.9%], F:4.9%, M:6.2%, n:978
L. fortune	1.67 Gb	32 Kb	312 Kb	C:81.9% [S:78.6%, D:3.27%], F:7.36%, M:10.73%, n:978
A. purpuratus	724.8 Mb	80 Kb	1.02 Mb	C:90.4% [S:89.5%, D:0.9%], F:3.9%, M:5.7%, n:978
P. yessoensis	988 Mb	38 Kb	804 Kb	C:94.0% [S:92.0%, D:2.0%], F:1.3%, M:4.7%, n:978
C. farreri	780 Mb	21.5 Kb	602 Kb	C:93.0% [S:90.9%, D:2.1%], F:2.4%, M:4.6%, n:978
P. fucata	991.02 Mb	21.4 Kb	59.02 Mb	C:87.3% [S:77.4%, D:9.9%], F:3.1%, M:9.6%, n:978
C. virginica	685 Mb	1.9 Mb	75.9 Mb	C:94.6% [S:91.9%, D:2.7%], F:1.1%, M:4.3%, n:978
C. gigas	558 Mb	31.2 Kb	401.7 Kb	C:86.9% [S:82.0%, D:4.9%], F:1.1%, M:12.0%, n:978
S. glomerate	796.5 Mb	39.4 Kb	804.2 Kb	C:91.6% [S:88.2%, D:3.4%], F:3.8%, M:4.6%, n:978
O. bimaculoides	2.34 Gb	5.5 Kb	475.1Kb	C:89.2% [S:88.7%, D:0.5%], F:3.6%, M:7.2%, n:978

L. gigantea	359 Mb	96 Kb	1.87Mb	C:95.7% [S:94.6%, D:1.1%], F:0.9%, M:3.4%, n:978

[†]*B. platifrons*, Bathymodiolus platifrons; *M. philippinarum,* Modiolus philippinarum; *L. fortune*, Limnoperna fortune; *A. purpuratus*, Argopecten purpuratus; *P. yessoensis*, Patinopecten yessoensis; *C. farreri*, Chlamys farreri; *C. virginica*, Crassostrea virginica; *C. gigas*, Crassostrea gigas; *S. glomerate*, Saccostrea glomerate; *O. bimaculoides*, Octopus bimaculoides; *L. gigantean*, Lottia gigantean; *P. fucata*, Pinctada fucata; C, complete BUSCOs; S, complete and single-copy BUSCOs; D, complete and duplicated BUSCOs; F, fragmented (partial) BUSCOs; M, missing BUSCOs; n, number of BUSCOs.

Table S32 Number of tyrosinase genes present in the genome of different species. Related to Figure 2.

Species	**Gene number**
Homo sapiens	1
Mus musculus	1
Gallus gallus	1
Xenopus tropicalis	1
Danio rerio	1
Octopus bimaculoides	7
Lottia gigantea	2
Crassostrea gigas	24
Patinopecten yessoensis	26
Pinctada fucata	31
Ruditapes philippinarum	21